NASA TN D-281



# TECHNICAL NOTE

D-281

## ANALYSIS OF TRAJECTORY PARAMETERS FOR PROBE AND ROUND-TRIP MISSIONS TO MARS

By James F. Dugan, Jr.

Lewis Research Center
Cleveland, Ohio

NATIONAL AERONAUTICS AND SPACE ADMINISTRATION

WASHINGTON June 1960

NATIONAL AERONAUTICS AND SPACE ADMINISTRATION

TECHNICAL NOTE D-281

# ANALYSIS OF TRAJECTORY PARAMETERS FOR PROBE AND ROUND-TRIP MISSIONS TO MARS

By James F. Dugan, Jr.

## SUMMARY

For one-way transfers between Earth and Mars, charts are obtained that show velocity, time, and angle parameters as functions of the eccentricity and semilatus rectum of the Sun-focused conic. From these curves are obtained others useful in planning one-way and round-trip missions to Mars. The analysis is characterized by circular coplanar planetary orbits, successive two-body approximations, impulsive velocity changes, and circular parking orbits at 1.1 planet radii. For round trips, the mission time considered ranges from 130 to 1000 days, while wait time spent in the parking orbit around Mars ranges from 0 to 454 days. Departure dates, one-way travel times, and individual velocity increments are presented for round trips requiring minimum total velocity increments.

For both single-pass and orbiting Martian probes, the time span available for launch becomes appreciable with only a small increase in velocity-increment capability above the minimum requirement. The effectiveness of velocity-increment increases in reducing travel time and Earth-Mars separation distance at probe arrival is less pronounced for orbiting probes than it is for single-pass probes. For round-trip missions with a specified wait time spent in orbit around Mars, the minimum total velocity increment does not decrease continuously as mission time increases.

## INTRODUCTION

In planning any space mission, a trajectory analysis is a prerequisite for deciding upon specific features of the mission. The analysis will show the interrelations among such parameters as departure date, elapsed time for separate phases of the mission, total mission time, individual and total velocity increments, and Earth-vehicle separation distance at different times during the mission. The velocity parameters

influence the choice of propulsion system and permit preliminary estimates of propellant requirements to be made. The time and separation-distance parameters are relevant to reliability and communication considerations.

Some of the trajectory information needed to plan various missions to Mars is found in references 1 to 5. However, discussion of some missions of interest is not to be found, and the behavior of some trajectory parameters required in planning Mars missions is either unavailable or inconvenient to calculate. For example, the Mars round-trip missions treated in these references do not include the direct-aphelion family of round trips that result in minimum total velocity increments for mission times of 600 to 1000 days. For many of the round trips, only values of mission time and total velocity increment are presented.

In this report, charts of the kind suggested by Vertregt in reference 6 are presented for one-way trajectories between Earth and Mars. These charts facilitate the preliminary planning of a particular mission, show the available choices, and give approximate values of launch date, duration of voyage, and required velocity increments. Modifications of these charts were used to find the interrelations among trajectory parameters of interest for many one-way single-pass, one-way orbiting, and round-trip missions between Earth and Mars.

The equations of reference 6 and several additional equations, needed to obtain parameters useful in round-trip calculations, were programed for a digital computer. Tables of trajectory-parameter data were obtained for trips between Earth and Mars. From these tables were constructed the trajectory charts suggested by Vertregt. In each chart, $\epsilon$ was plotted against $p$ for constant values of each trajectory parameter of interest ($\epsilon$ and $p$ are the eccentricity and semilatus rectum of the Sun-focused vehicle conic).

Working curves, in which the trajectory parameter of interest appears as the ordinate, were then used to obtain pertinent information on a wide range of one-way and round-trip missions between Earth and Mars. For single-pass and orbiting Martian probes, the relations among launch date, travel time, required velocity increment, and Earth-Mars separation distance when the probe arrives at Mars are presented. Missions requiring minimum velocity increment are discussed. By graphical procedures, the round trips requiring minimum total velocity increment are found for wait times spent in the parking orbit at Mars of 0, 100, and 454 days. The variations of launch date, travel time, and individual velocity increment with mission time are presented for 0- and 100-day wait times.

Because of the simplifying assumptions that are made in the analysis, all values of launch date, duration of mission, and required velocity increments presented in this report are approximate. The results should be used only in the preliminary planning of a particular mission. For more exact values, an analysis based on the n-body equations of motion and a three-dimensional model of the solar system should be used. In spite of their approximate nature, the results of this analysis do show the interrelations among the important trajectory parameters and should serve as a useful guide in making more precise calculations.

## ANALYSIS

### Assumptions

The following simplifying assumptions were made:

(1) The planets describe circular orbits around the Sun. The orbits of Mars and the space vehicle lie in the plane of the ecliptic.

(2) The vehicle is attracted by only one inverse-square central force field at a time. When "near" a planet, the vehicle is attracted by the planet. When "far" from the planets, it is attracted by the Sun.

(3) Most of the voyage is unpowered. The time during which thrust is applied to the vehicle is insignificant compared with the total duration of the voyage; that is, the impulsive-velocity-increment concept is used.

(4) The travel time spent under the influence of the planets is negligible compared with the travel time spent under the influence of the Sun.

### Possible Heliocentric Trajectories

In traveling between Earth and Mars (or any two planets), an infinite number of Sun-focused conic sections can be traversed. For a given ellipse, which will in general intersect the orbits of Earth and Mars at four points, four alternate routes can be considered (fig. 1(a)). (A list of symbols appears in appendix A; fig. 1(b) aids in defining some of the trajectory angles.) The direct route D from Earth to Mars is along 1-2, the perihelion route P along 4-1-2, the aphelion route A along 1-2-3, and the indirect route I along 4-1-2-3. If the ellipse is tangent to Earth's orbit (fig. 1(a)), routes D and P become identical and also routes A and I. Similarly, if the ellipse is tangent to Mars' orbit, routes D and A become identical, and also

routes P and I. For a given parabolic or hyperbolic path, only direct and perihelion routes are possible.

## Eccentricity - Semilatus-Rectum Charts

In reference 6 Vertregt shows how interplanetary trajectory parameters along all possible conics can be expressed as functions of the radius of the destination planet's orbit and the eccentricity and semimajor axis of the Sun-focused conic. In an addendum to reference 6, it is pointed out that a considerable simplification results from constructing trajectory diagrams in which eccentricity is plotted against semilatus rectum (instead of semimajor axis) for constant values of trajectory parameters. One $\epsilon$-p diagram for Earth-Venus trajectories is included by Vertregt to illustrate the advantages.

The equations from reference 6 and several additional equations, needed to obtain parameters useful in round-trip calculations, were programed for a digital computer. Tables of trajectory-parameter data were obtained for trips between Earth and Mars. The procedure for calculating these tables is discussed in appendix B. From the tables were constructed $\epsilon$-p trajectory charts such as those shown in figures 2(a) to (c). A wide range of useful trajectories is shown within the arbitrary boundaries of $p_{max} = 3.0$ and $\epsilon_{max} = 2.0$. A complete set of 22 $\epsilon$-p charts for Earth-Mars trajectories can be obtained by sending in the card at the back of this report. The trajectory parameters included in these charts are $\Delta v_E$, $\Delta v_M$, $(\Delta v_E + \Delta v_M)$, $V_E$, $V_M$, $(V_E + V_M)$, $T_D$, $T_P$, $T_A$, $T_I$, $\psi_D$, $\psi_P$, $\psi_A$, $\psi_I$, $\lambda_D$, $\lambda_P$, $\lambda_A$, $\lambda_I$, $\varphi_1$, $\varphi_2$, $\alpha_1$, and $\alpha_2$.

## Probe Missions

In finding the interrelations among trajectory parameters of interest for specific Earth-Mars missions, it was found convenient to use working curves in which the various parameters of interest are plotted against eccentricity for constant values of semilatus rectum. (These curves are not included in the report, since they depict the same information as contained in the $\epsilon$-p charts.) Because the procedure for treating the one-way single-pass missions is very similar to that for the one-way orbiting missions, only the former is discussed. For one-way single-pass missions from Earth to Mars, four trajectory parameters are singled out as being of special interest: (1) velocity increment required near Earth when starting from a circular parking orbit of 1.1 Earth radii, (2) travel time, (3) configuration angle at departure, and (4) Earth-Mars separation distance at arrival. Configuration angle at departure defines launch date (fig. 2(d)). The Hohmann date is defined as that date on with Mars' heliocentric longitude is greater than Earth's

by 44.4°, this being the configuration required for a Hohmann transfer from Earth to Mars.

For a given value of $\Delta v_E$, values of $\epsilon$ and p are read from the working curve, $\Delta v_E$ against $\epsilon$ for constant p. These values of $\epsilon$ and p permit values of $\psi_1$ and T to be read from their respective working curves. The value of configuration angle when the probe arrives at Mars is calculated from

$$\psi = \psi_1 + (\dot{\varphi}_E - \dot{\varphi}_M)\Delta t \tag{1}$$



where

$$\dot{\varphi}_E = 0.9856 \text{ deg/day}$$

$$\dot{\varphi}_M = 0.5240 \text{ deg/day}$$

and

$$\Delta t = T$$

Earth-Mars separation distance at arrival can then be read from figure 2(e), which is a plot of

$$d = \left(R_E^2 + R_M^2 - 2R_E R_M \cos \psi\right)^{1/2} \tag{2}$$

where

$$R_E = 92{,}900{,}000 \text{ miles}$$

and

$$R_M = 141{,}600{,}000 \text{ miles}$$

These data are then plotted as T against $\psi_1$ for constant $\Delta v_E$ (fig. 3(a)) and d against $\psi_1$ for constant $\Delta v_E$ (fig. 3(b)).

## Round-Trip Missions

For round-trip missions to Mars, it is convenient to introduce an angle parameter $\lambda$ defined by

$$\lambda_i = \varphi_i - \dot{\varphi}_E T_i \tag{3}$$

Therefore, $\lambda$ is the angular difference between the vehicle's travel and Earth's travel during a one-way trip between planet orbits. The relation that must be satisfied during a round-trip mission to Mars with a wait time $T_w$ spent in orbit around Mars is

$$\lambda_{out} + (\dot{\Phi}_M - \dot{\Phi}_E)T_w + \lambda_{back} = N360 \qquad (4)$$

where N can be 0 or $\pm$ an integer. The outgoing and return trajectories can be combined in an infinite number of combinations involving direct, perihelion, aphelion, and indirect routes.



To illustrate the technique employed for the round-trip missions, consider the combinations involving direct and perihelion routes. For a specific value of $\lambda_D$, values of $\epsilon_D$ and $p_D$ are read from the $\lambda_D$ working curve. Values of $(\Delta v_E + \Delta v_M)$ and $T_D$ are then read for one pair of $\epsilon_D$ and $p_D$ values. For a specific value of $T_w$, the value of $\lambda_P$ is calculated from equation (4). The $\lambda_P$ working curve yields pairs of values for $\epsilon_P$ and $p_P$. For each pair, values of $(\Delta v_E + \Delta v_M)_P$ and $T_P$ are read from their working curves. The total velocity increments and total mission times are calculated, and $\Delta v_T$ is plotted against $T_T$. A curve can be drawn for each pair of $\epsilon_D, p_D$ values. The envelope of these curves forms a single curve for a specific $\lambda_D$ value. The procedure is repeated for many $\lambda_D$ values so that an envelope curve for the direct-perihelion round trips can be drawn.

By repeating the whole procedure for other combinations of D, P, A, and I routes, the minimum total velocity increment required to accomplish a round trip of given duration and given wait time at Mars can be found.

## RESULTS AND DISCUSSION

For all three types of mission considered, emphasis is placed upon the interrelations among velocity parameters, travel times, vehicle-planet separation distance, and planetary configuration angle at departure, which is equivalent to departure date (see fig. 2(d)).

### Single-Pass Probes

The interrelations among trajectory parameters for a single-pass Martian probe launched from an orbit of 1.1 Earth radii are shown in figure 3. The contours are lines of constant velocity increment. Dashed lines, which converge at the point representing a Hohmann path, separate

the plot into four regions representing direct, perihelion, aphelion, and indirect routes. Along each dashed line, the Sun-focused conic section is tangent to either Earth's or Mars' orbit, and the route is either direct or indirect (see fig. 1(a)). For instance, the dashed line between the perihelion routes and the indirect routes represents indirect routes along a Sun-focused ellipse that is tangent to Mars' orbit.



The straight dash-dot line forming the arbitrary upper right boundary of the diagram (fig. 3(a)) can be interpreted in two ways. In the conventional way, it shows the relations among travel time, velocity increment at Earth, and configuration angle at departure. The second interpretation is that it represents Hohmann paths. In this instance only, the ordinate represents the sum of two time intervals - the Hohmann travel time of 259 days and the time interval between the date indicated by the abscissa and the next date at which a Hohmann path could be flown. By waiting for the next Hohmann date before firing, the required velocity increment is reduced to the Hohmann value 2.19 miles per second, and the probe arrives at Mars on the same date as it would for the conventional interpretation.

Figure 3(a) indicates that, for a given velocity increment, minimum travel time occurs for a direct route. Since the Hohmann path is indicated by a point, departure can occur only at one instant of time during the synodic period of 780 days. Even a small increase in probe velocity increment above the Hohmann value results in an appreciable time span during which launch is possible. For example, the range of configuration angle at departure for a velocity-increment capability only 440 feet per second higher than the Hohmann value is $-56^{\circ}$ to $-28^{\circ}$. This corresponds to a launch span of about 2 months.

The same increase in velocity increment above the Hohmann value can diminish the Earth-Mars separation distance at arrival from 148 to 97 million miles (fig. 3(b)). Further increases in velocity-increment capability permit probe arrivals at Mars when the separation distance is the minimum value, 49 million miles.

Of special interest are the paths requiring minimum velocity increments for travel times less than the Hohmann value of 259 days (fig. 4). Increasing the probe velocity-increment capability 2200 feet per second above the Hohmann value decreases travel time from 259 to 130 days and Earth-Mars separation distance at arrival from 148 to 63 million miles.

## Orbiting Probes

The relations among trajectory parameters for an orbiting Martian probe are shown in figure 5. The probe is assumed to be launched from

a parking orbit at 1.1 Earth radii with the terminal parking orbit at 1.1 Mars radii. Because two impulses are required for such a mission, the velocity parameter employed is the sum of the velocity increments required to leave the orbit around Earth and enter the orbit around Mars. The features of the orbiting probe trajectories are similar to those for the single-pass probe. Direct routes result in minimum travel time for a given velocity-increment capability. Increasing the velocity-increment capability of the probe above the Hohmann value increases the time span during which departure is possible and decreases the Earth-Mars separation distance at probe arrival.



In figure 6 minimum total-velocity-increment data are shown for travel times less than 259 days. In order to decrease travel time from 259 to 130 days, velocity-increment capability of the probe must increase from 3.49 to 5.69 miles per second (fig. 6(a)). For such an increase, Earth-Mars separation distance at arrival would decrease from 148 to 87 million miles (fig. 6(b)).

For vehicles having thrust to weight ratios less than about $10^{-1}$, the amount of propellant required for a mission cannot be estimated from velocity-increment values. Propellant estimates for these vehicles can be made, however, from values of hyperbolic velocity, vehicle thrust to weight ratio, propellant specific impulse, planetary gravitational force constant, and parking-orbit radius (ref. 7). Since the amount of propellant increases as hyperbolic velocity increases, trajectory data for minimum hyperbolic velocity are of interest. Such trajectories result in near minimum propellant expenditures and thus are useful in preliminary mission planning.

The effect of minimizing hyperbolic velocity rather than impulsive velocity increment is shown in figure 7. The hyperbolic velocities are made dimensionless by dividing by the Earth's mean orbital speed of 18.5 miles per second. For a given travel time, the Sun-focused path resulting in minimum hyperbolic velocity is different from that resulting in minimum total velocity increment. This is borne out by comparing figure 6 with figure 7. For example, the launch dates for a 130-day trip differ by 18 days (figs. 6(c) and 7(d)), while Earth-Mars separation distance upon arrival differs by 9 million miles (figs. 6(b) and 7(e)). It is well to remember that travel time refers to the time the unpowered vehicle is under the influence of the Sun; that is, it is the time required to travel from the orbit of Earth to the orbit of Mars. Since the time spent in spiraling around the planets can be quite long, the actual travel time can be considerably longer than that shown. For missions requiring propulsion power all or most of the time, of course, the curves shown here do not apply.

## Round Trips

The round-trip mission to Mars begins with the space vehicle in orbit about the Earth at 1.1 Earth radii. The first velocity increment sends the vehicle on the outgoing trajectory from Earth to Mars. A second velocity increment settles the vehicle into an orbit about Mars at 1.1 Mars radii. After a specified wait time ranging from 0 to 454 days, a third velocity increment sends the vehicle on its return trajectory from Mars to Earth. The final velocity increment causes the vehicle to orbit Earth at 1.1 Earth radii. Total velocity increment is the sum of the four impulsive velocity increments, while mission time is the sum of the travel times for the outward and return trajectories and the specified wait time spent in the parking orbit about Mars.

The specification of parking orbits at 1.1 planet radii is arbitrary. If atmospheric braking is used, the propellant expenditure required to attain parking orbits on round-trip missions is reduced greatly. The features of optimum round-trip missions employing atmospheric braking will change markedly from those discussed in this report.

Minimum-total-velocity-increment variations with mission time. - Outgoing and return trajectories can be combined in an infinite number of combinations involving direct, perihelion, aphelion, and indirect routes. Particular combinations lead to envelope curves such as those shown in figure 8 for a wait time at Mars of 0 days. For a given mission time, the total velocity increment shown is the minimum value attainable using the designated combination of outward and return trajectories. An envelope of the curves shown in figure 8 gives the minimum total velocity increments required for mission times ranging from 130 to 1000 days. Direct-direct round trips yield minimum total velocity requirements for mission times of 152 days and less. From 152 to about 400 days, combinations of direct and perihelion routes should be used. Perihelion-perihelion round trips are best for missions lasting 400 to 558 days. Between 558 and 605 days, the combination is labeled perihelion-indirect and also indirect-indirect. This is so because one path is along an ellipse tangent to Mars' orbit. As pointed out in the ANALYSIS, in such a case route P becomes identical with route I and route D becomes identical with route A (fig. 1(a)). The fact that direct-aphelion and aphelion-aphelion round trips are best for missions between 605 and 800 days indicates again that one route is along an ellipse tangent to Mars' orbit. For missions lasting 800 to 1000 days, indirect routes both ways give minimum total velocity requirements.

It is noteworthy that the total velocity increment does not decrease continuously as mission time increases. This would seem to rule out missions of certain duration. For example, missions lasting between 500 and 675 days require total velocity increments equal to or greater

than that required for a 500-day mission. The trip having the least total velocity increment (9.9 miles/sec) requires the long mission time (799 days). A trip of a year's duration requires the higher total velocity increment of 14.2 miles per second.

The effect of wait time at Mars on total velocity increment and mission time is shown in figure 9. Portions of the curves from figure 8 for zero days' wait at Mars are replotted in figure 9. The right branch is for mission times from 600 to 800 days, while the left branch is for mission times from 152 to 558 days. For the right branch, as wait time at Mars increases the curve is displaced toward longer mission times and lower total velocity increments. The right terminus of the curve for 454 days' wait at Mars represents a round trip in which both outward and return trajectories are along the Hohmann ellipse. A mission time of 972 days is compatible with the minimum total velocity increment of 6.98 miles per second. The effect of wait time on the left branch is different. As wait time at Mars increases, the curve is displaced toward longer mission times but higher total velocity increments. For 100 days' wait at Mars, an 845-day mission is compatible with the least total velocity increment, 9.4 miles per second. To shorten the mission time to 465 days, a total velocity increment of 17.0 miles per second is required.

For a given mission time and wait time at Mars, other trajectory parameters besides total velocity increment are of interest. Among these are the individual velocity increments comprising the total, the time required for outward and return trajectories, and the configuration angle required to begin the mission. The variation of these parameters with wait time at Mars will be shown for round trips of special significance. For convenience, the discussion is divided into that pertaining to round trips employing direct and aphelion routes and that pertaining to round trips employing direct and perihelion routes.

Round trips employing direct and aphelion routes. - In figure 10 is shown the effect of a tangency restriction on total velocity increment and mission time for direct-aphelion round trips. The dashed curves are for round trips restricted to outward and return trajectories that are tangent either to Earth's or Mars' orbit (fig. 1(a)). The solid curves represent the minimum total velocity increment required for a range of mission times and wait times at Mars of 0 (fig. 10(a)) and 454 days (fig. 10(b)). For some missions, the tangency restriction imposes a large penalty on total velocity increment. From figure 10(a), the total velocity increment required for a 680-day mission increases from 13.2 to 17.1 miles per second when tangent trajectories are specified. However, for round trips requiring the least total velocity increment (9.9 miles/sec for 0 days' wait and 6.98 miles/sec for 454 days' wait), one trajectory is along the Hohmann ellipse and the other is along the aphelion branch of an ellipse tangent to Earth's orbit.

For direct-aphelion round trips requiring the least total velocity increments, trajectory-parameter variations with wait time at Mars are shown in figure 11. Mission time is seen to increase more slowly than wait time (fig. 11(a)). As wait time at Mars increases from 0 to 100 days, mission time increases from 800 to only 845 days. The rate at which total velocity increment decreases as wait time increases is almost constant (fig. 11(b)). Increasing the wait time at Mars by 100 days lowers the total velocity increment 0.65 mile per second. Three of the four velocity increments composing the total are relatively constant for the range of wait times from 0 to 454 days (fig. 11(c)). The fourth velocity increment varies from 3.80 to 1.30 miles per second. Since one leg of the round trip is along the Hohmann ellipse, one of the travel times is constant at 259 days (fig. 11(d)). The other ranges from 540 down to 259 days. Because either trajectory can be selected for the outward path, each round trip could commence on a Hohmann date. For a particular round trip of interest, the Earth-Mars separation distance during the wait time spent in orbit around Mars can be found from equation (1) and figure 2(e).

In figures 12 and 13 are shown trajectory-parameter variations useful in planning round-trip missions to Mars of about 600 to 800 days' duration. Round-trip data for 0 days' wait in a parking orbit at Mars are presented in figure 12. Wait time is 100 days for figure 13.

Round trips employing direct and perihelion routes. - Round trips employing direct and perihelion routes are interesting in that they result in shorter missions at the expense of higher total velocity increments (see, DD, PP, and DP curves in fig. 8). The effect of the tangency restriction on the direct-perihelion round trips is shown in figure 14 for wait times at Mars of 0 (fig. 14(a)) and 100 days (fig. 14(b)). The dashed and solid curves have the same meaning as discussed in connection with figure 10. While the effect of the tangency restriction on the total velocity increment can be large, it is quite small for missions requiring near minimum total velocity increment. For 0 days' wait at Mars (fig. 14(a)), a tangency point at 440 days and 13.85 miles per second compares with an envelope point of 435 days and 13.60 miles per second. For 100 days' wait (fig. 14(b)), a tangency point at 500 days and 17.10 miles per second compares with an envelope point at 490 days and 16.75 miles per second. Thus, the minimum-total-velocity-increment data based on the tangency restriction closely approximate the true minimum-total-velocity-increment data.

Trajectory data for the former round trips are shown in figure 15. One path is along the direct branch of an ellipse tangent to Earth's orbit, while the other is along the perihelion branch of an ellipse tangent to Mars' orbit. Total mission time and total velocity increment increase almost linearly with wait time at Mars (figs. 15(a) and (b)).

To attain 100 days of waiting time, mission time must increase 70 days and total velocity increment 3.30 miles per second. For the full range of wait time, one of the trajectories remains fixed (fig. 15(c)) - the direct path along an ellipse tangent to Earth's orbit. The largest velocity increment by far is that required near Earth for a perihelion path along an ellipse tangent to Mars' orbit. The path that remains fixed for all wait times requires a configuration angle of -42° (fig. 15(d)) and a travel time of 169 days (fig. 15(e)).

Direct-perihelion and perihelion-perihelion round trips are contrasted in figure 16. For a wait time at Mars of 0 days, decreasing mission time from 400 to 200 days calls for an increase in total velocity increment from 13.8 to 24.0 miles per second. For 100 days' wait at Mars, decreasing mission time from 500 to 300 days requires an increase in total velocity increment from 16.6 to 32.8 miles per second. In these ranges of mission time, direct-perihelion round trips yield minimum total velocity increments. At higher mission times, perihelion-perihelion round trips should be used. Other trajectory parameters of interest for the round trips of figure 16 are shown in figures 17 to 20. The parameters are configuration angle, the four velocity increments composing the total, and the two travel times for the outward and return trajectories. The information in these figures is useful in planning round-trip missions to Mars of about 150 to 600 days' duration.

## CONCLUDING REMARKS

The analysis of trajectory parameters for probe and round-trip missions to Mars has revealed some interesting features. For probes that pass near Mars only once, the time span available for launch is appreciable even for a small increase in velocity-increment capability above the minimum requirement of 11,560 feet per second. A velocity-increment increase of only 2200 feet per second can be used to decrease travel time from 259 to 130 days and Earth-Mars separation distance at arrival from 148 to 63 million miles.

For probes that orbit around Mars, again, the time span available for launch is appreciable even for small increases in velocity-increment capability above the minimum requirement. However, the effectiveness of velocity-increment increases in reducing travel time and separation distance is less pronounced. An increase in velocity increment of 63 percent above the minimum requirement is necessary to shorten travel time 50 percent and Earth-Mars separation distance at arrival 41 percent.

For round-trip missions to Mars, total mission time is minimized by combining one direct route with another only when the velocity-increment capability is the very high value of 28.5 miles per second or

more. At lower values, perihelion and aphelion routes must be used to minimize total mission time. For 0 days' wait at Mars, the total velocity increment required for a 365-day mission is 14.2 miles per second. A 799-day mission requires 9.9 miles per second. For 100 days' wait at Mars, the total velocity increment required for a 465-day mission is 17 miles per second. An 845-day mission requires 9.4 miles per second. For a given wait time spent in orbit around Mars, total velocity increment does not decrease continuously as mission time increases. For example, missions lasting between 500 and 675 days with 0 days' wait at Mars require total velocity increments equal to or greater than that required for a 500-day mission.

E-737

Lewis Research Center
National Aeronautics and Space Administration
Cleveland, Ohio, March 1, 1960

# APPENDIX A

## SYMBOLS

| | |
|---|---|
| A | aphelion route (see fig. 1(a)) |
| D | direct route (see fig. 1(a)) |
| d | Earth-Mars separation distance at arrival, $10^6$ miles |
| I | indirect route (see fig. 1(a)) |
| N | an integer (eq. (4)) |
| n | ratio of mean radius of destination planet's orbit around the Sun to that of Earth |
| P | perihelion route (see fig. 1(a)) |
| p | semilatus rectum of heliocentric conic section, A.U. |
| q | semimajor axis of heliocentric ellipse or hyperbola, A.U. |
| R | mean distance of planet from Sun, miles |
| T | heliocentric travel time, days |
| $T_W$ | waiting time in parking orbit at Mars, days |
| $\Delta t$ | time interval, days |
| V | ratio of hyperbolic velocity to mean orbital velocity of Earth, (miles/sec)/(18.5 miles/sec) |
| v | velocity, miles/sec or ft/sec |
| $\Delta v$ | velocity increment, miles/sec or ft/sec |
| $\alpha$ | heliocentric trajectory angle relative to circumferential direction (see fig. 1(b)), deg |
| $\epsilon$ | eccentricity of heliocentric conic section |
| $\lambda$ | angular difference between vehicle's travel and Earth's travel during one-way trip between planet orbits (eq. (3)), deg |

$\tau$ angle (see eq. (B3c)), radians

$\varphi$ angular position of vehicle measured counterclockwise from perihelion of heliocentric conic section (see fig. 1(b)), deg

$\dot{\varphi}$ angular velocity of planet, deg/day

$\psi$ configuration angle (see fig. 1(b)), deg

Subscripts:

A aphelion route

c circular

D direct route

E Earth

e escape

I indirect route

i index signifying A, D, I, or P

j index signifying 1 or 2

M Mars

max maximum

min minimum

P perihelion route

T total

1 intersection of heliocentric conic section with Earth's orbit

2 intersection of heliocentric conic section with Mars' orbit

# APPENDIX B

## TRAJECTORY-PARAMETER CALCULATION PROCEDURE

The trajectory-parameter calculation procedure is based mainly on the equations presented in reference 6. These and several additional equations were programed for a digital computer to yield trajectory-parameter tables with $p$ and $\epsilon$ as arguments for values of $n \lesseqgtr 1.0$. The initial value of $p$ is set equal to 0.1. The minimum value of $\epsilon$ is calculated from equation (B1a) or (B1b), whichever yields the larger value:

$$\epsilon_{min} = \pm(p - 1) \qquad \left.\begin{array}{l} + \text{ for } n > 1.0 \\ - \text{ for } n < 1.0 \end{array}\right\} \qquad \text{(B1a)}$$

or

$$\epsilon_{min} = \pm(1 - p/n) \qquad \text{(B1b)}$$

The value of $n$ for Earth-Mars trajectories is 1.5237.

The $p$-$\epsilon$ pair of values $(0.1, \epsilon_{min})$ defines a specific Sun-focused conic section, and all trajectory parameters can be expressed as functions of only $p$ and $\epsilon$. The nondimensional hyperbolic velocities are calculated from

$$V_1 = \left(3 - 2\sqrt{p} - \frac{1 - \epsilon^2}{p}\right)^{1/2} \qquad \text{(B2a)}$$

$$V_2 = \left(\frac{3 - 2\sqrt{\frac{p}{n}}}{n} - \frac{1 - \epsilon^2}{p}\right)^{1/2} \qquad \text{(B2b)}$$

The velocity increments required to leave the parking orbit around Earth and to enter the parking orbit around Mars are calculated from the following equations derived from the constant-energy property of two-body motion:

$$\Delta v_E = \left[(18.50\ V_1)^2 + (v_{e,E})^2\right]^{1/2} - v_{c,E} \qquad \text{(B2c)}$$

$$\Delta v_M = \left[(18.50\ V_2)^2 + (v_{e,M})^2\right]^{1/2} - v_{c,M} \qquad \text{(B2d)}$$

At both Earth and Mars, parking orbits of 1.1 planet radii were assigned. The values of $v_{e,E}$, $v_{c,E}$, $v_{e,M}$, and $v_{c,M}$ used in the calculations were 6.624, 4.683, 3.010, and 2.128 miles per second, respectively.

While the velocity parameters are independent of route, the travel times are different for direct, perihelion, aphelion, and indirect routes. Moreover, the equation for travel time for a direct route changes form depending on whether $\epsilon$ is less than, equal to, or greater than 1.0.

For $\epsilon < 1.0$,

$$T_D = \pm 58.13\, q^{3/2}\left[(\tau_1 - \tau_2) - \epsilon(\sin\tau_1 - \sin\tau_2)\right]\begin{cases} + & \text{for } n < 1 \\ - & \text{for } n > 1 \end{cases} \tag{B3a}$$

where

$$q = \frac{p}{1 - \epsilon^2} \tag{B3b}$$

$$\tau_1 = \cos^{-1}\left(\frac{q - 1}{q\epsilon}\right) \tag{B3c}$$

$$\tau_2 = \cos^{-1}\left(\frac{q - n}{q\epsilon}\right) \tag{B3d}$$

The equation for $\epsilon = 1.0$ was not programed. As a result of using $p$ rather than $q$ in the diagrams (see fig. 2), the curves run continuously from the area of ellipses ($\epsilon < 1.0$), through the line of parabolas ($\epsilon = 1.0$), to the area of the hyperbolas ($\epsilon > 1.0$).

For $\epsilon > 1.0$,

$$T_D = \pm 58.13\, q^{3/2}\left[\epsilon(\sinh\tau_1 - \sinh\tau_2) - (\tau_1 - \tau_2)\right]\begin{cases} + & \text{for } n < 1 \\ - & \text{for } n > 1 \end{cases} \tag{B3e}$$

where

$$q = \frac{p}{\epsilon^2 - 1} \tag{B3f}$$

$$\tau_1 = \cosh^{-1}\left(\frac{q+1}{q\epsilon}\right) \tag{B3g}$$

$$\tau_2 = \cosh^{-1}\left(\frac{q+n}{q\epsilon}\right) \tag{B3h}$$

The travel times for perihelion, aphelion, and indirect routes are calculated from

$$T_P = T_D + 116.26\, q^{3/2}(\tau_j - \epsilon \sin \tau_j) \begin{cases} j = 1 & \text{for } n > 1 \\ j = 2 & \text{for } n < 1 \end{cases} \tag{B3i}$$

$$T_A = T_D + 116.26\, q^{3/2}(\pi - \tau_j + \epsilon \sin \tau_j) \begin{cases} j = 1 & \text{for } n < 1 \\ j = 2 & \text{for } n > 1 \end{cases} \tag{B3j}$$

$$T_I = 365.26(q^{3/2} - T_D) \tag{B3k}$$

Because aphelion and indirect routes are not possible for hyperbolic orbits, travel times for these routes are calculated only for values of $\epsilon < 1.0$.

The change in heliocentric angle also depends on the route:

$$\varphi_1 = \cos^{-1}\left[\frac{q(1-\epsilon^2) - 1}{\epsilon}\right] \tag{B4a}$$

$$\varphi_2 = \cos^{-1}\left[\frac{q(1-\epsilon^2) - n}{n\epsilon}\right] \tag{B4b}$$

$$\varphi_D = |\varphi_2 - \varphi_1| \tag{B4c}$$

$$\varphi_P = \varphi_1 + \varphi_2 \tag{B4d}$$

$$\varphi_A = 360 - \varphi_P \qquad \text{for } \epsilon < 1.0 \tag{B4e}$$

$$\varphi_I = 360 - \varphi_D \qquad \text{for } \epsilon < 1.0 \tag{B4f}$$

Since configuration angle depends on both travel time and change in heliocentric angle, it depends on the route also:

$$\psi_i = \frac{0.9856}{n^{3/2}} T_i - \varphi_i \tag{B5}$$

Another trajectory parameter depending on both $T$ and $\varphi$ is $\lambda$, which is useful in round-trip calculations (see eqs. (3) and (4)):

$$\lambda_i = \varphi_i - 0.9856\ T_i \tag{B6}$$

The trajectory parameter $\alpha$ is calculated from

$$\alpha_1 = \tan^{-1} \frac{\pm\epsilon \sin \varphi_1}{1 + \epsilon \cos \varphi_1} \tag{B7a}$$

$$\alpha_2 = \tan^{-1} \frac{\pm\epsilon \sin \varphi_2}{1 + \epsilon \cos \varphi_1} \tag{B7b}$$

where plus is for $n > 1.0$ and minus is for $n < 1.0$.

Having calculated all trajectory parameters of interest for $p = 0.1$ and $\epsilon_{min}$, the value of $\epsilon$ is increased just enough to make it divisible by $\Delta\epsilon$. In the present calculations, $\Delta\epsilon$ is set equal to 0.1. With $p = 0.1$ and $\epsilon$ increased, all trajectory parameters are calculated. The procedure is repeated, the last calculation being for $p = 0.1$ and $\epsilon = 2.0$. At this point, the value of $p$ is increased by $\Delta p$. Again, the increment is set equal to 0.1. For $p = 0.2$, $\epsilon_{min}$ is calculated and all trajectory parameters are computed for this pair of $p$-$\epsilon$ values. The procedure is repeated until a stipulated range of the arguments $p$ and $\epsilon$ is covered. For the Earth-Mars calculations, $p$ ranges from 0.1 to 3.0 in increments of 0.1, and $\epsilon$ ranges from $\epsilon_{min}$ to 2.0 in increments of 0.1.

## REFERENCES

1. Ehricke, K. A., Whitlock, C. M., Chapman, R. L., and Purdy, C. H.: Calculations on a Manned Nuclear Propelled Space Vehicle. Rep. 532-57, Am. Rocket Soc., Inc., Dec. 1957.

2. Moeckel, W. E.: Interplanetary Trajectories with Excess Energy. Paper Presented at Int. Astronautical Cong., Amsterdam (Holland), Aug. 23-30, 1958.

3. Battin, R. H.: The Determination of Round-Trip Planetary Reconnaissance Trajectories. Rep. R-219, Instrumentation Lab., M.I.T., Jan. 1959.

4. Karrenberg, Hans K., and Arthur, Paul D.: Interplanetary Ballistic Orbits. Rep. 870-59, Am. Rocket Soc., Inc., June 1959.

5. Johnson, P. G., and Smith, R. L.: Round Trip Trajectories for Mars Observation. Paper presented at Nat. Meeting of Am. Astronautical Soc., Los Angeles (Calif.), Aug. 4-5, 1959.

6. Vertregt, M.: Interplanetary Orbits. Jour. British Interplanetary Soc., vol. 16, no. 6, Mar.-Apr. 1958, pp. 326-354.

7. Moeckel, W. E.: Trajectories with Constant Tangential Thrust in Central Gravitational Fields. NASA TR R-53, 1960.

| | Route | Earth to Mars | Mars to Earth |
|---|---|---|---|
| D | Direct | 1-2 | 3-4 |
| P | Perihelion | 4-1-2 | 3-4-1 |
| A | Aphelion | 1-2-3 | 2-3-4 |
| I | Indirect | 4-1-2-3 | 2-3-4-1 |

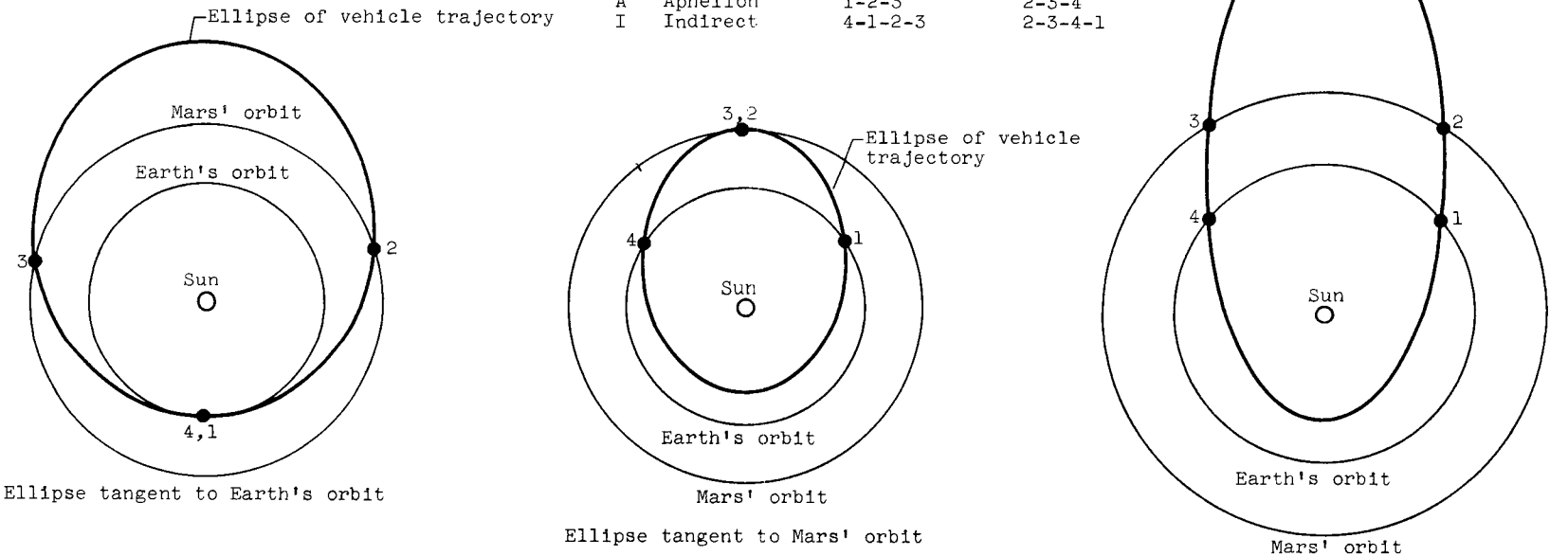


(a) Interplanetary routes.

Figure 1. - Nomenclature.

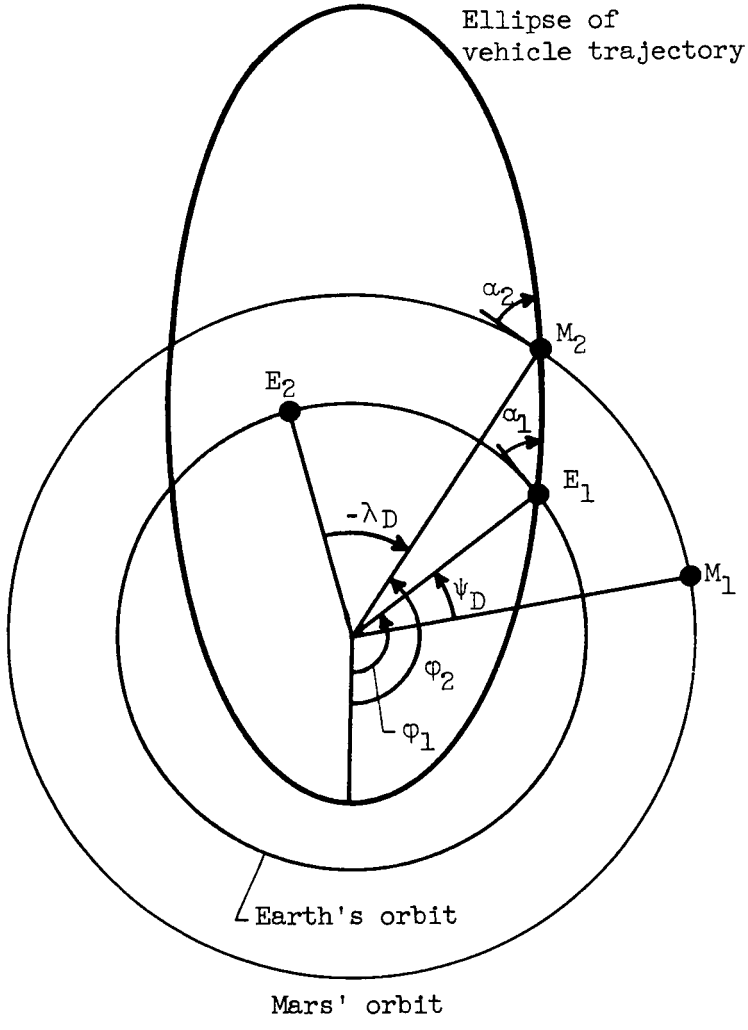


(b) Trajectory angles.

Figure 1. - Concluded. Nomenclature.

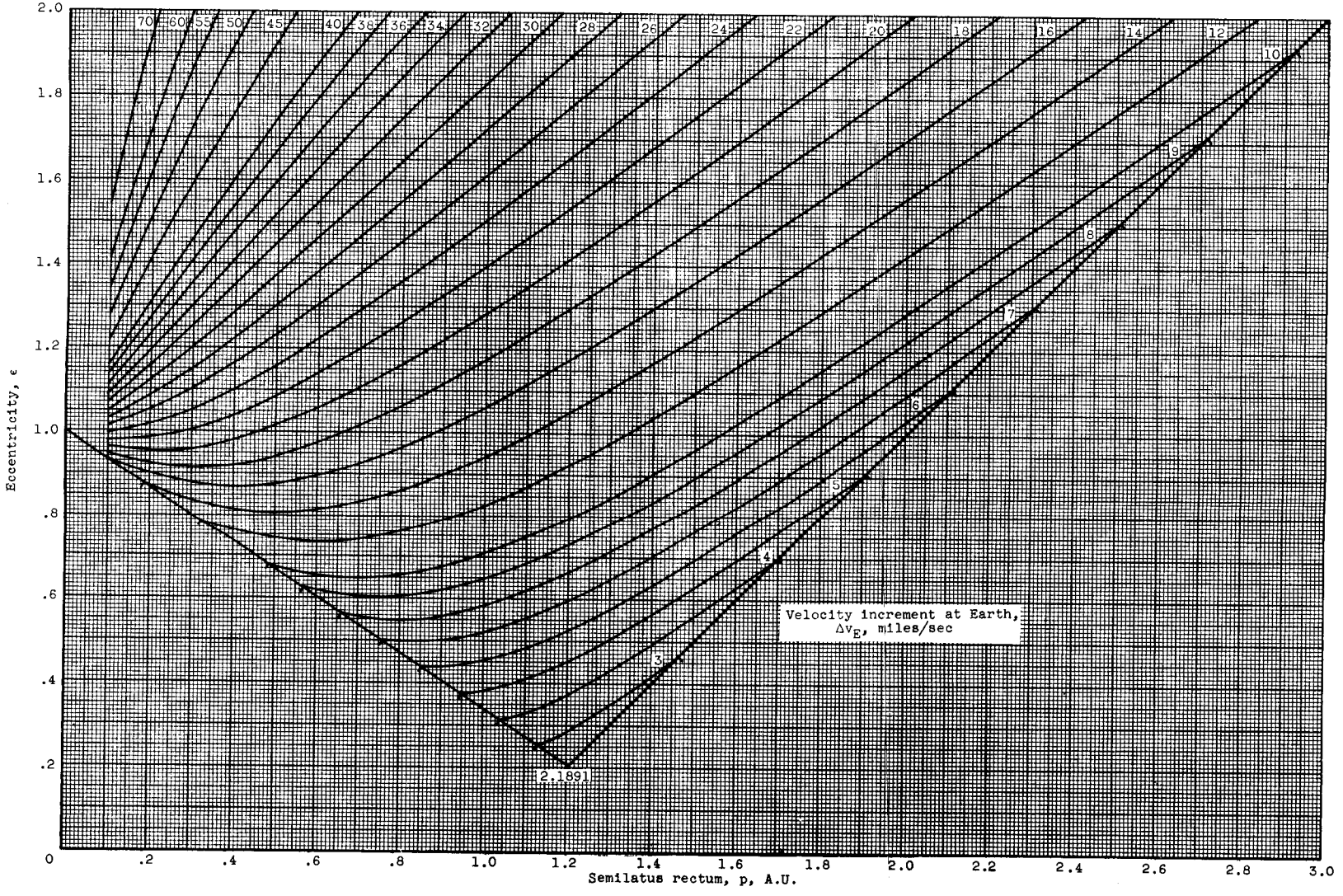


(a) Velocity increment at Earth.

Figure 2. - Trajectory parameters for trip between Earth and Mars. (A complete set of 22 ε-p charts for Earth-Mars trajectories can be obtained by using the request card bound in the back of this report.)

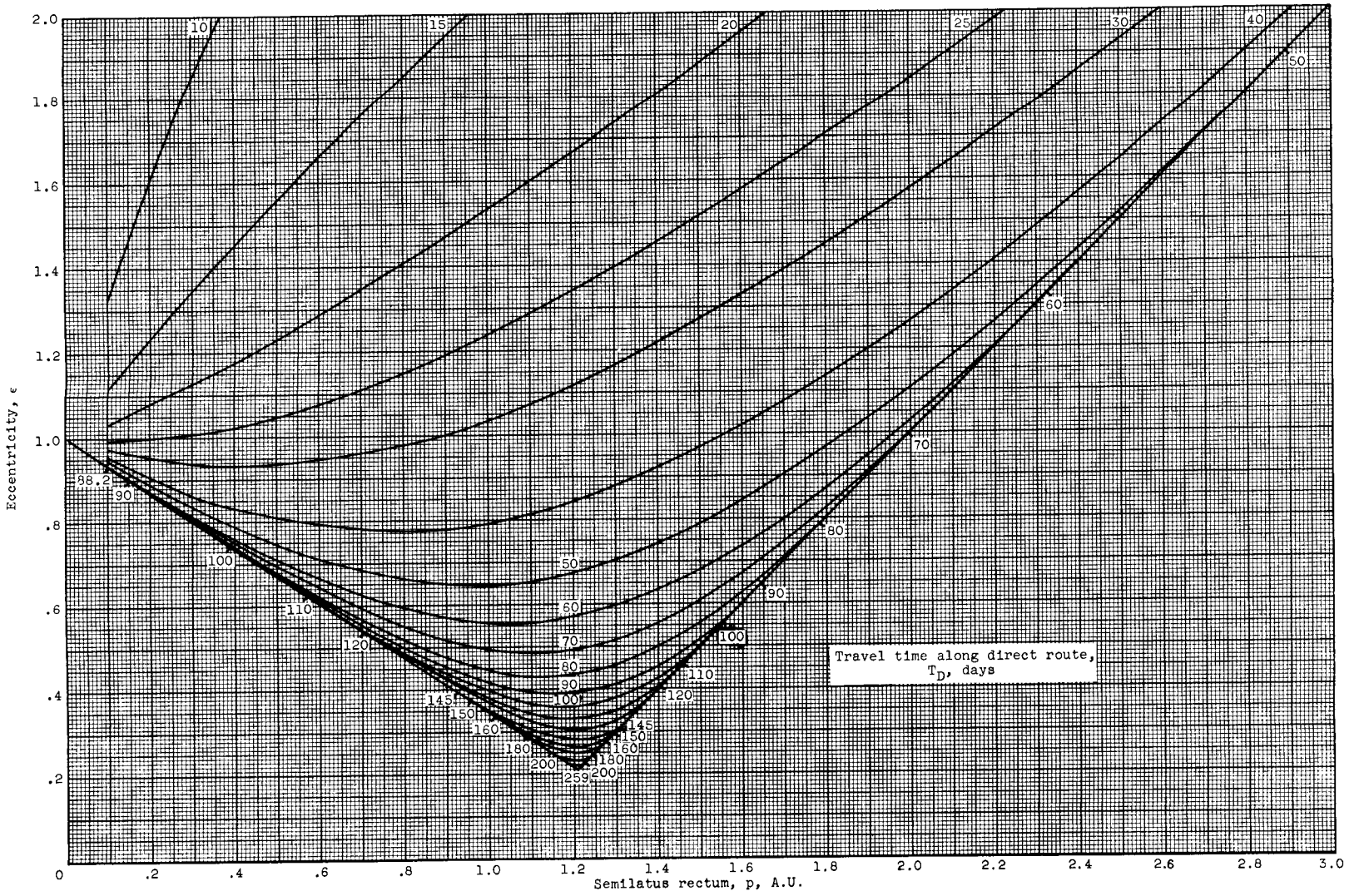


(b) Travel time for direct route.

Figure 2. - Continued. Trajectory parameters for trip between Earth and Mars.

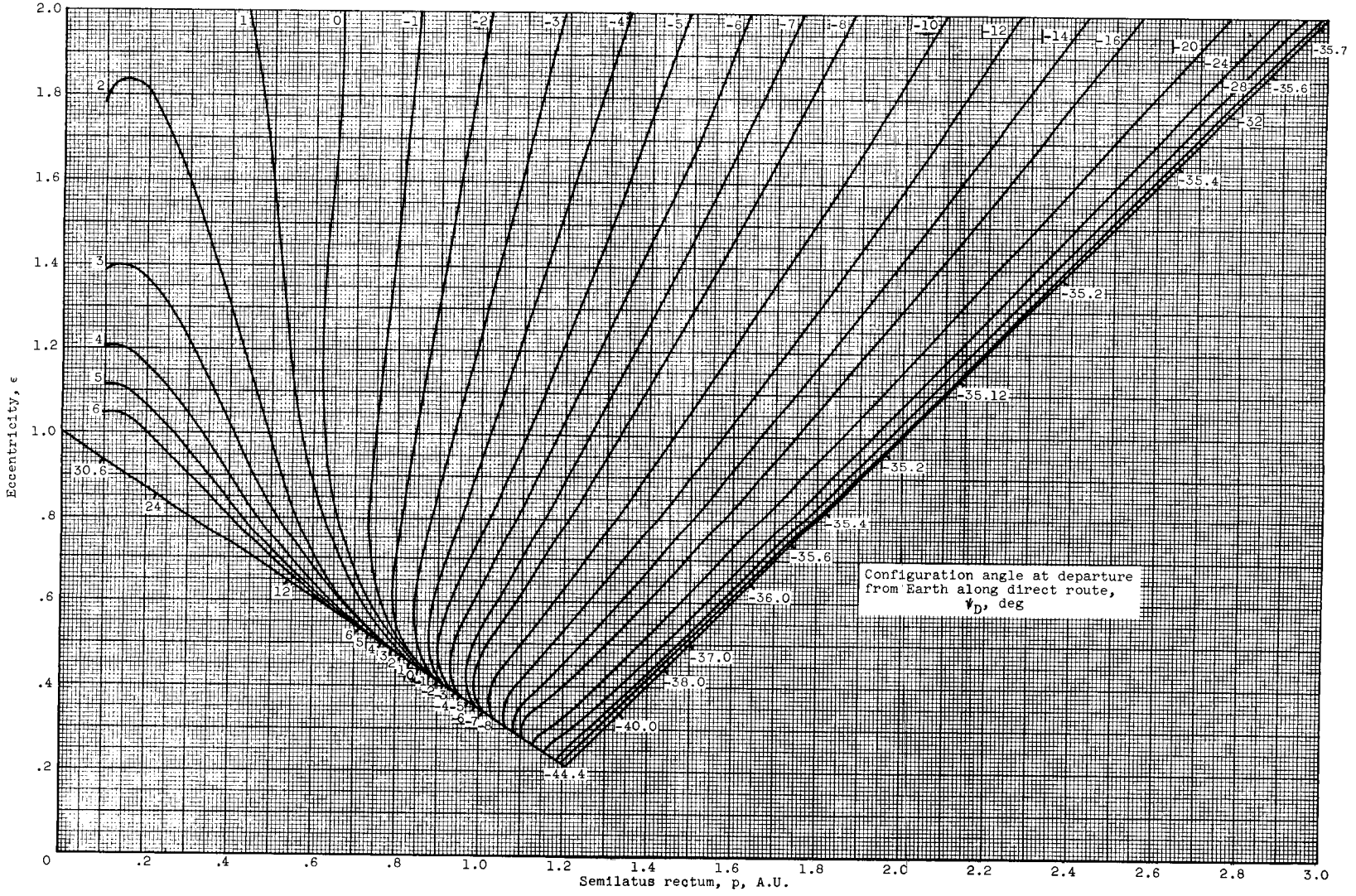


(c) Configuration angle at departure from Earth along direct route.

Figure 2. - Continued. Trajectory parameters for trip between Earth and Mars.

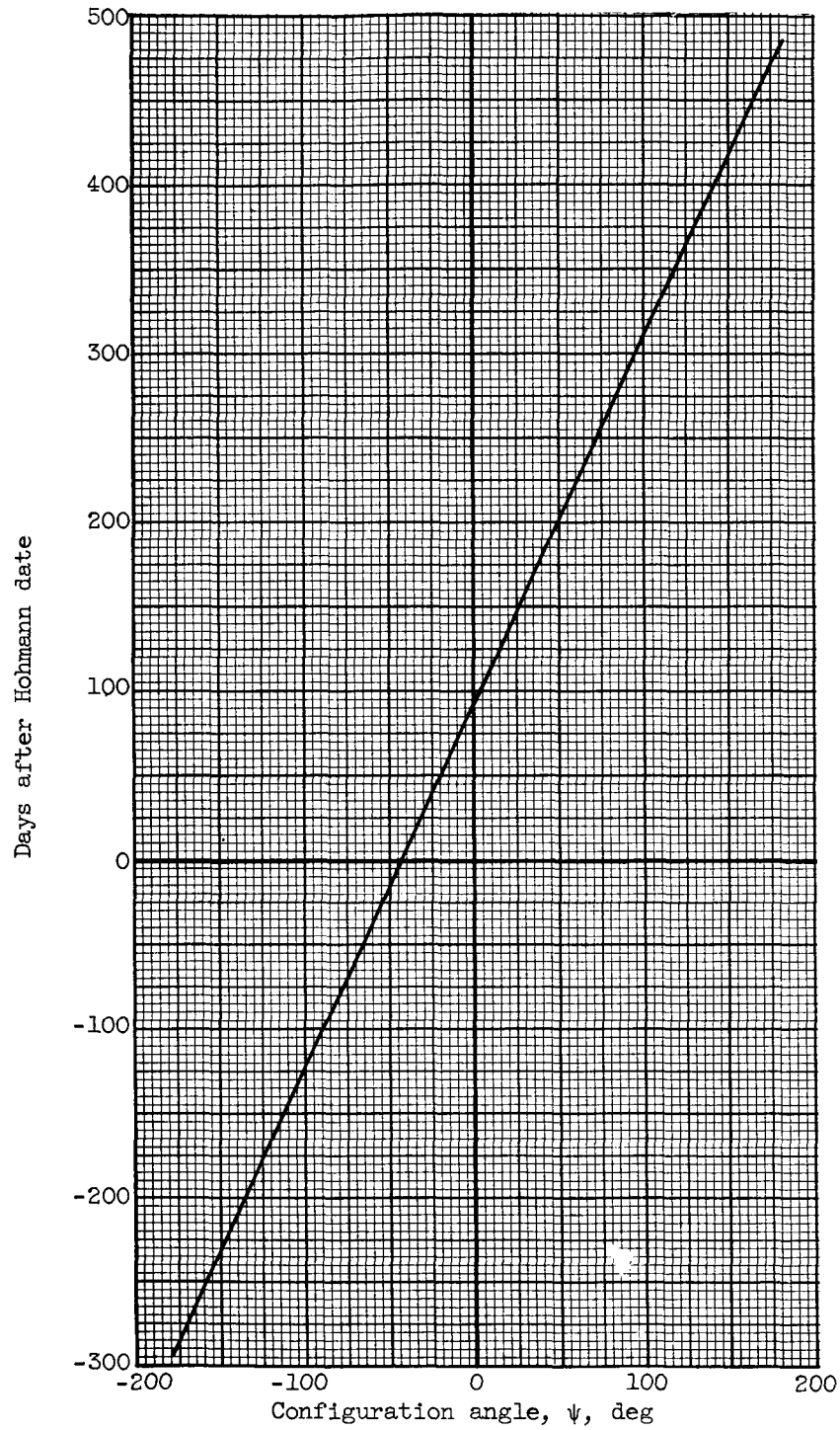


(d) Relation between date and configuration angle of Earth relative to Mars.

Figure 2. - Continued. Trajectory parameters for trip between Earth and Mars.

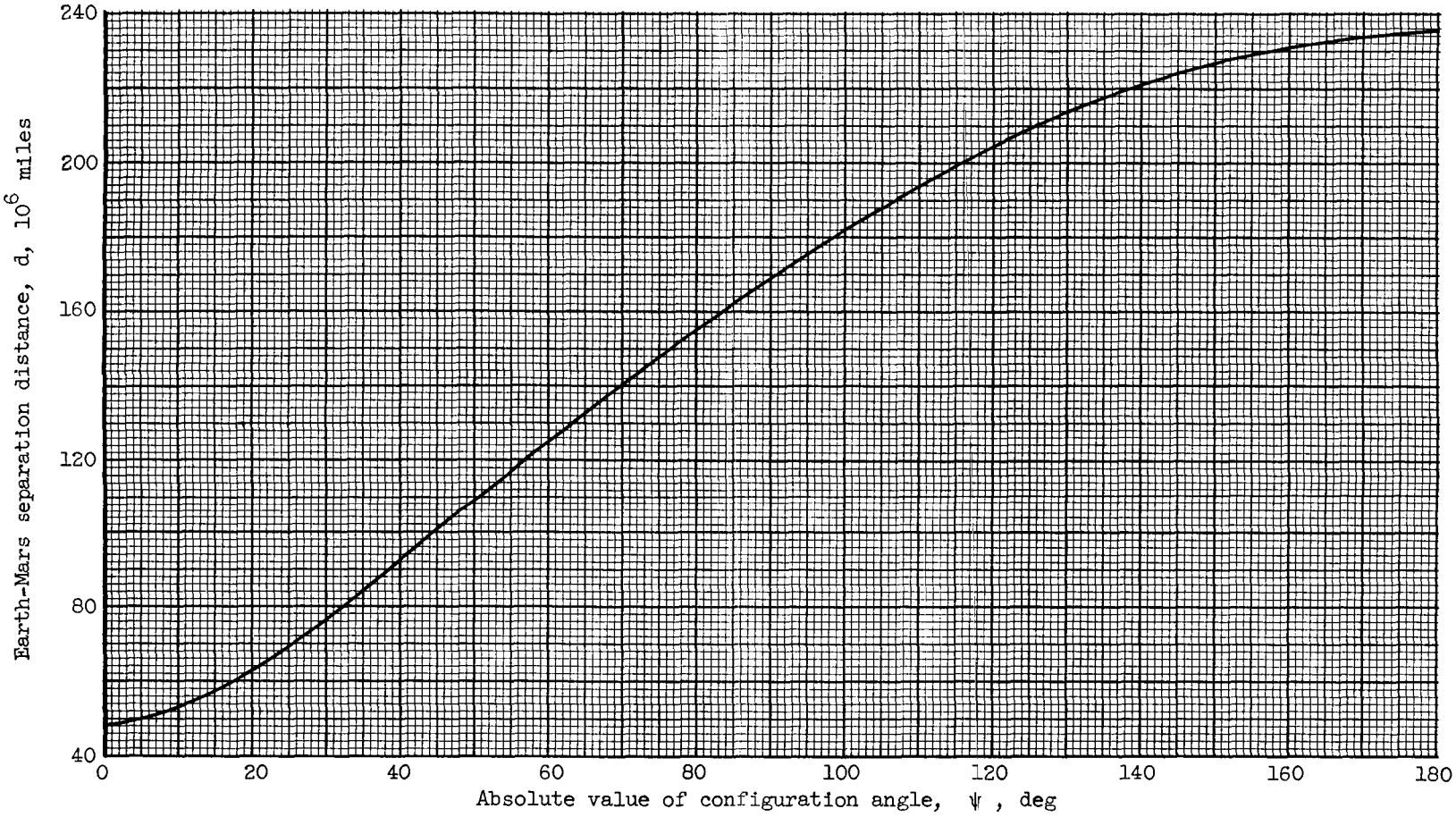


(e) Earth-Mars separation distance.

Figure 2. - Concluded. Trajectory parameters for trip between Earth and Mars.

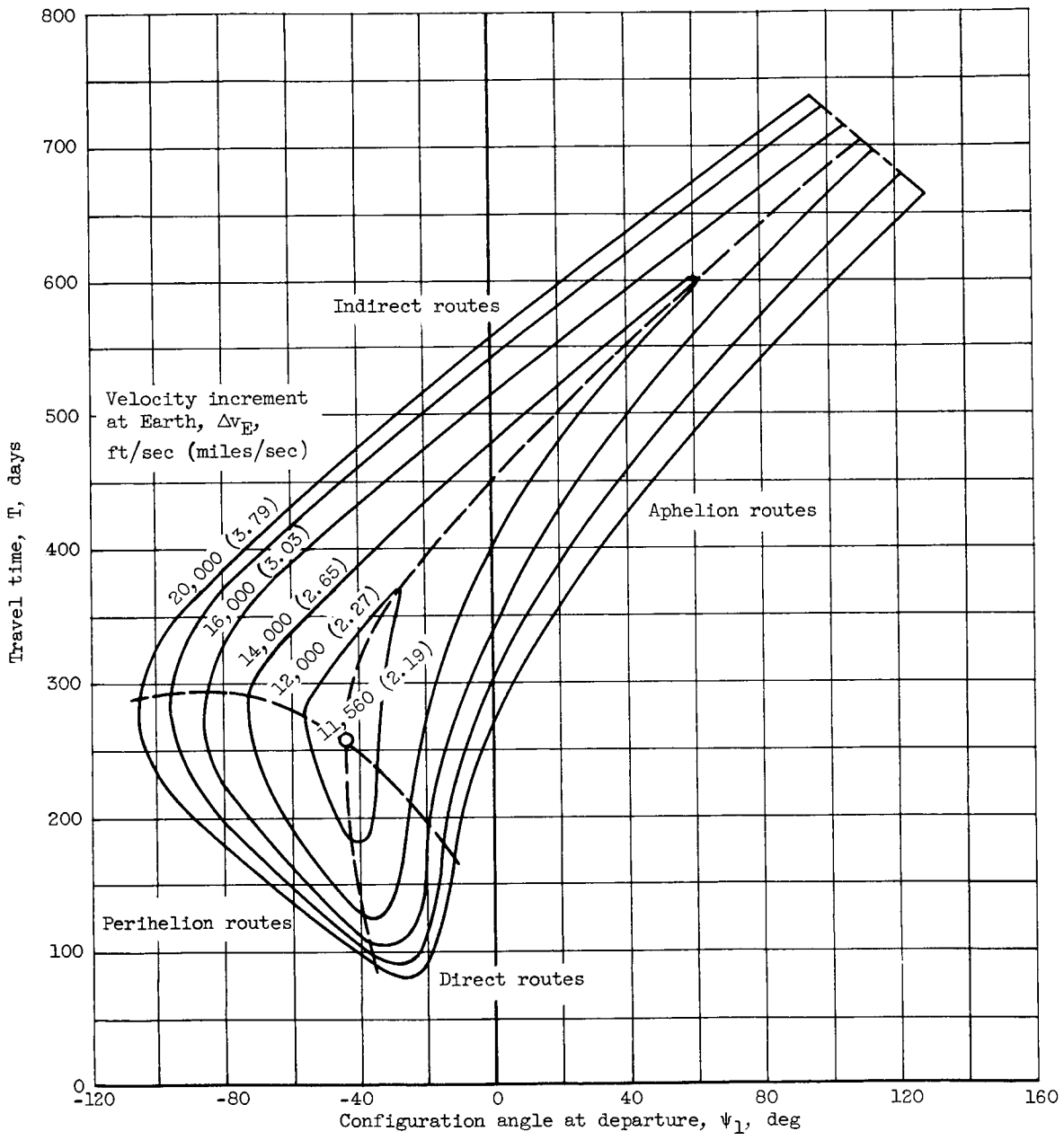


(a) Travel time, configuration angle at departure, and velocity increment at Earth.

Figure 3. - Path parameters for single-pass Martian probe launched from an orbit of 1.1 Earth radii.

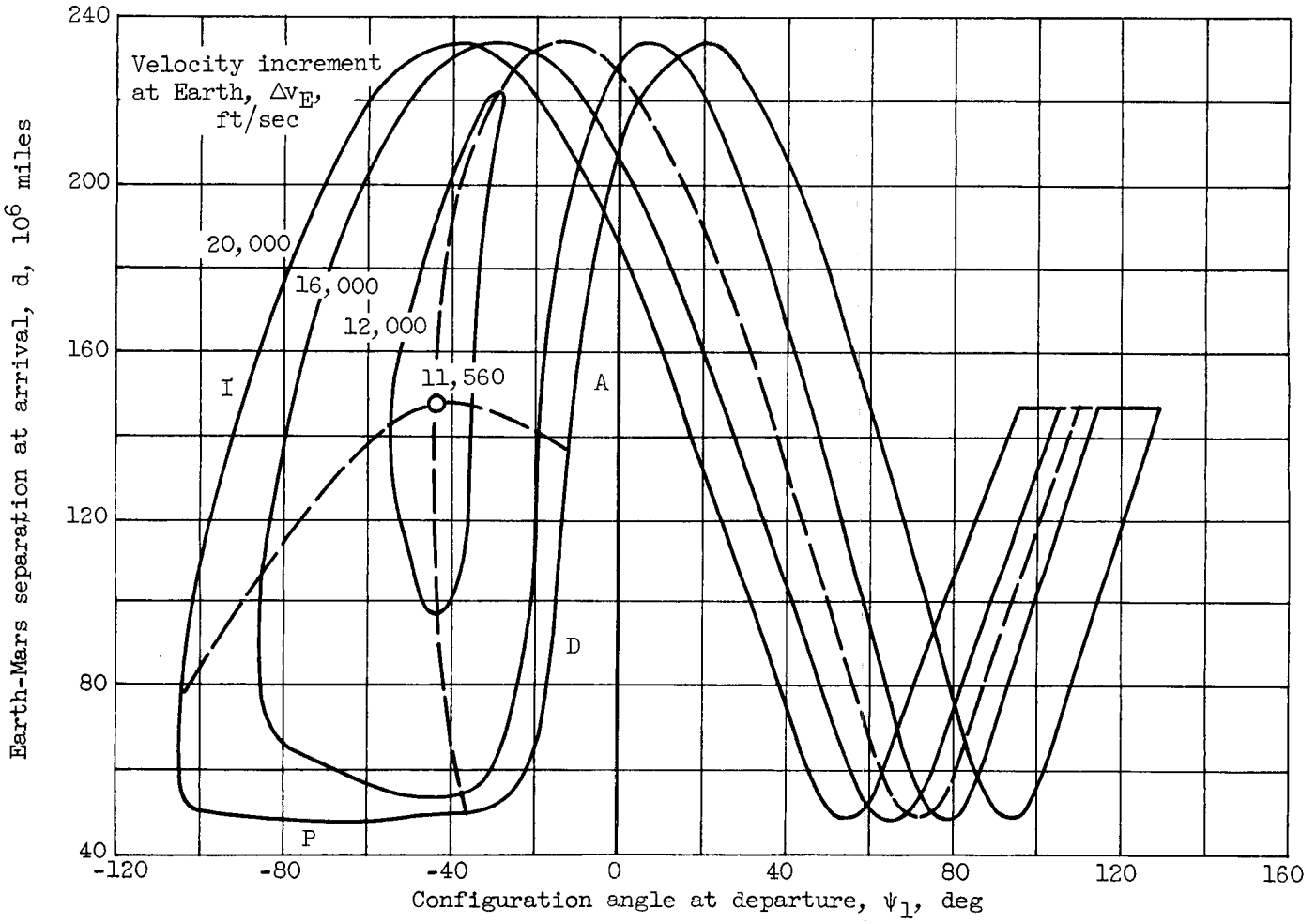


(b) Earth-Mars separation at arrival, configuration angle at departure, and velocity increment at Earth.

Figure 3. - Concluded. Path parameters for single-pass Martian probe launched from an orbit of 1.1 Earth radii.

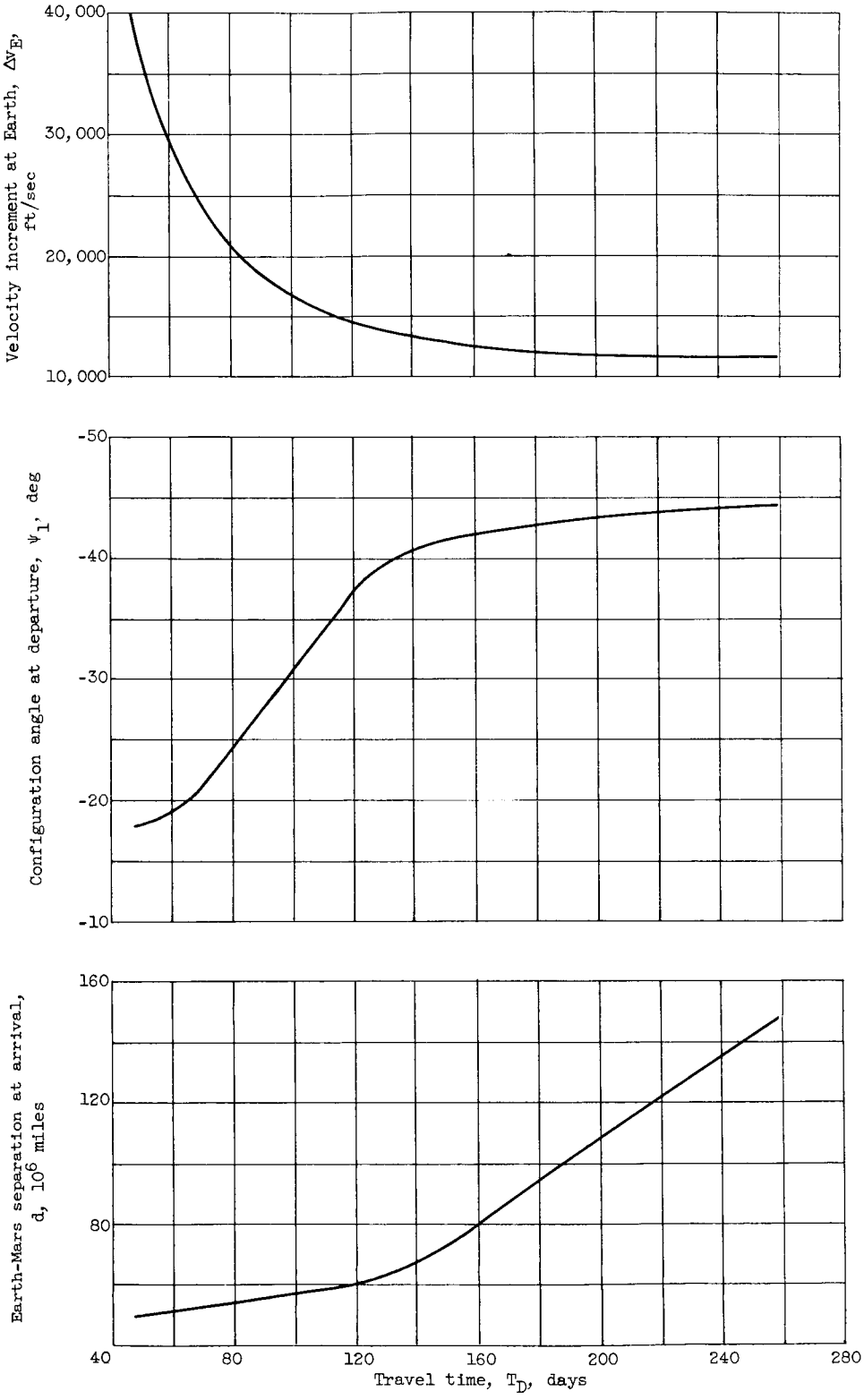


Figure 4. - Path parameters for single-pass Martian probe launched from an orbit of 1.1 Earth radii for minimum velocity increment.

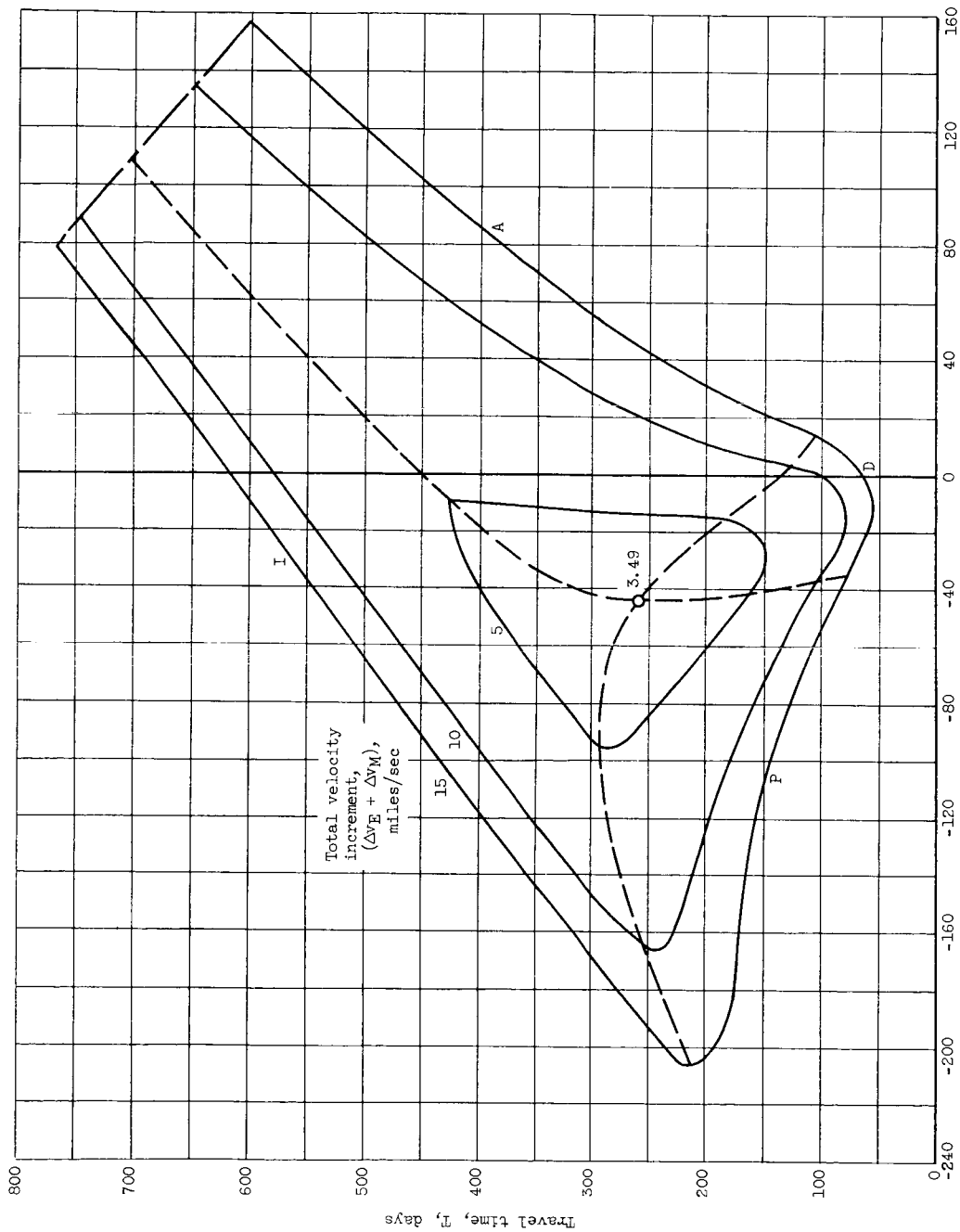


(a) Travel time, configuration angle at departure, and total velocity increment.

Figure 5. - Path parameters for an orbiting Martian probe launched from an orbit of 1.1 Earth radii. Terminal orbit is at 1.1 Mars radii.

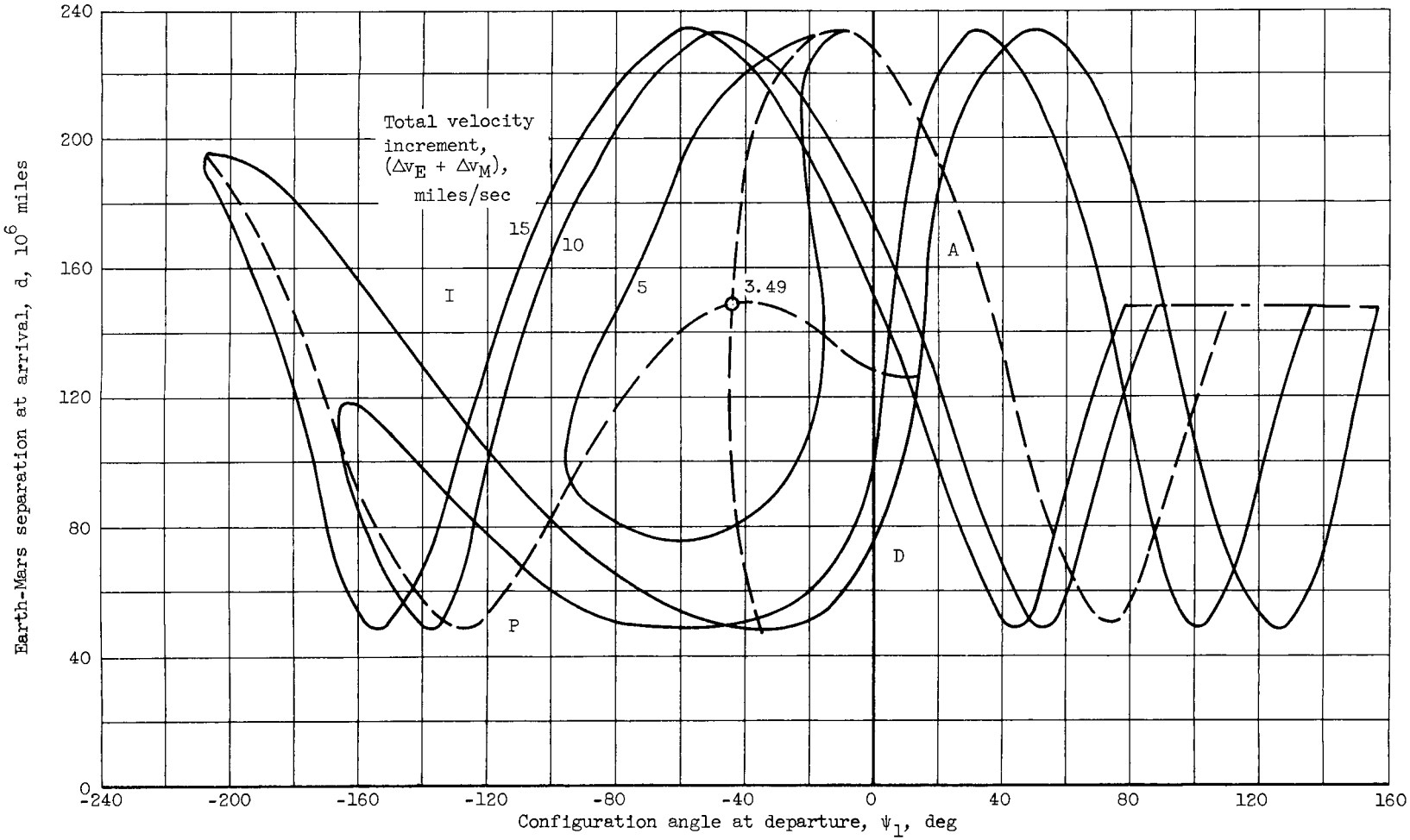


(b) Earth-Mars separation at arrival, configuration angle at departure, and total velocity increment.

Figure 5. - Concluded. Path parameters for an orbiting Martian probe launched from an orbit of 1.1 Earth radii. Terminal orbit is at 1.1 Mars radii.

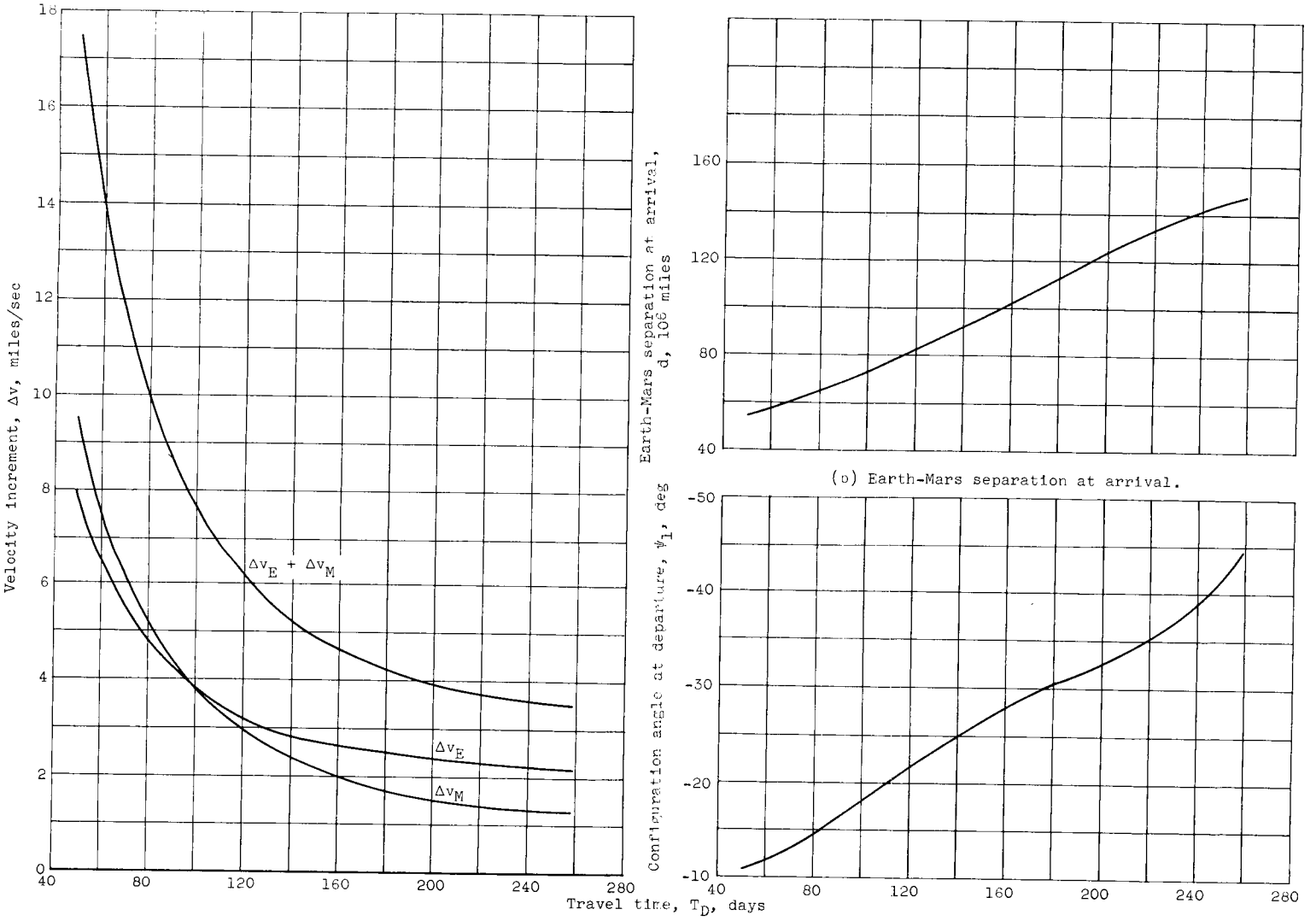


(a) Velocity increments.

(b) Earth-Mars separation at arrival.

(c) Configuration angle at departure.

Figure 6. - Path parameters for an orbiting Martian probe launched from an orbit of 1.1 Earth radii. Terminal orbit is at 1.1 Mars radii. Data for minimum total velocity increment.

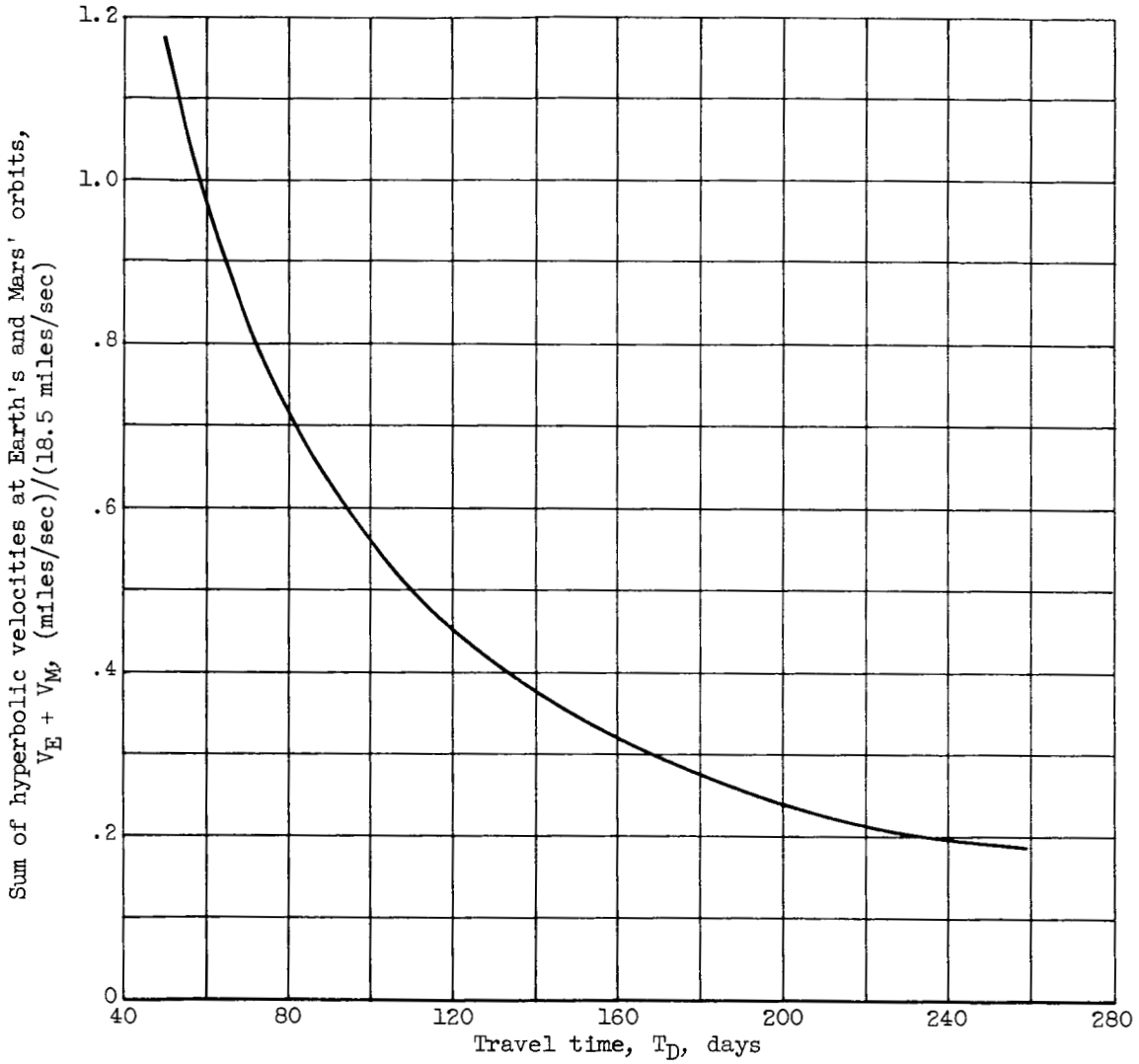


(a) Sum of hyperbolic velocities at Earth's and Mars' orbits.

Figure 7. - Path parameters for an orbiting Martian probe launched from an orbit of 1.1 Earth radii. Terminal orbit is at 1.1 Mars radii. Data for minimum sum of hyperbolic velocities at Earth's and Mars' orbits.

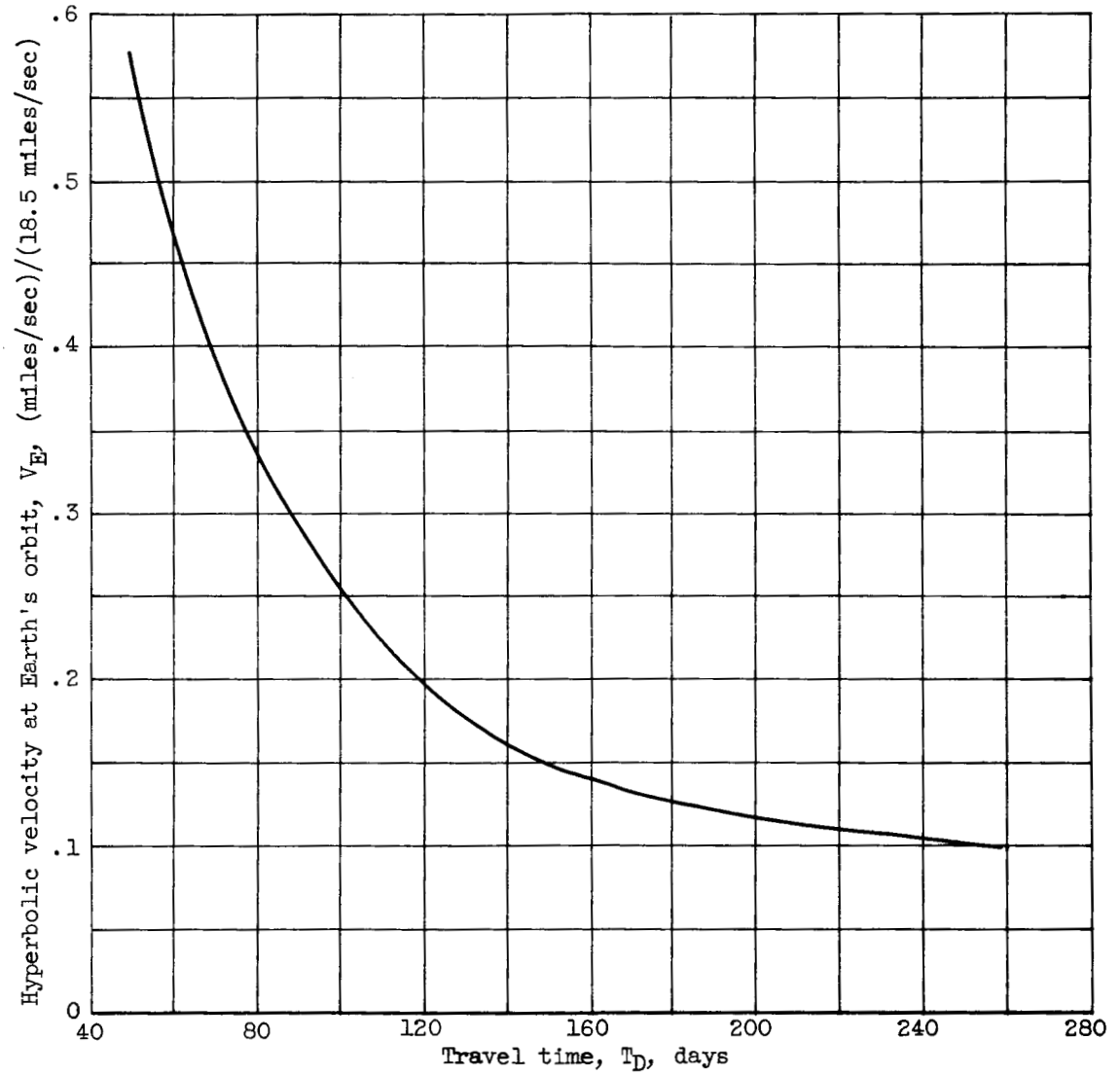


(b) Hyperbolic velocity at Earth's orbit.

Figure 7. - Continued. Path parameters for an orbiting Martian probe launched from an orbit of 1.1 Earth radii. Terminal orbit is at 1.1 Mars radii. Data for minimum sum of hyperbolic velocities at Earth's and Mars' orbits.

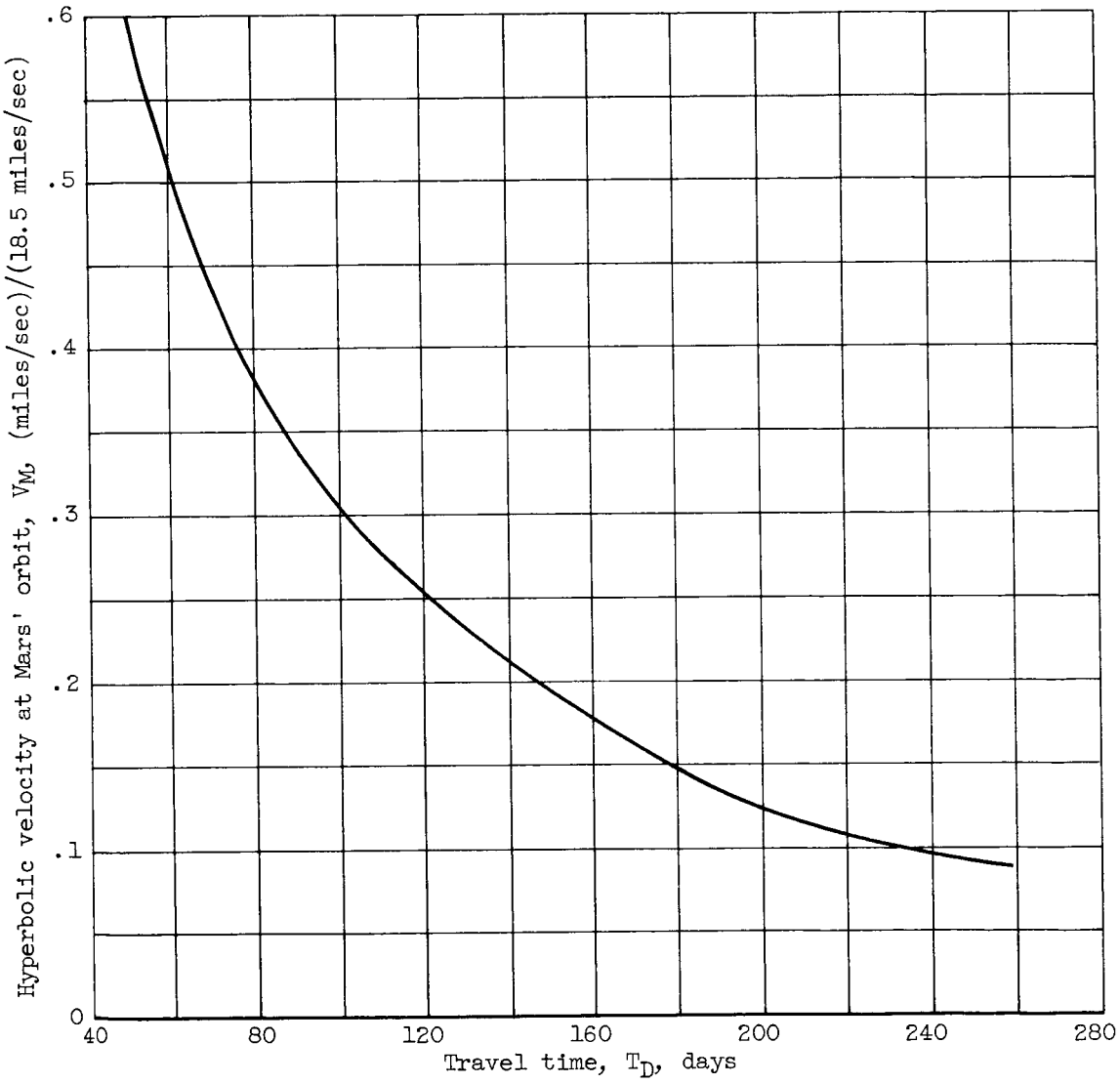


(c) Hyperbolic velocity at Mars' orbit.

Figure 7. - Continued. Path parameters for an orbiting Martian probe launched from an orbit of 1.1 Earth radii. Terminal orbit is at 1.1 Mars radii. Data for minimum sum of hyperbolic velocities at Earth's and Mars' orbits.

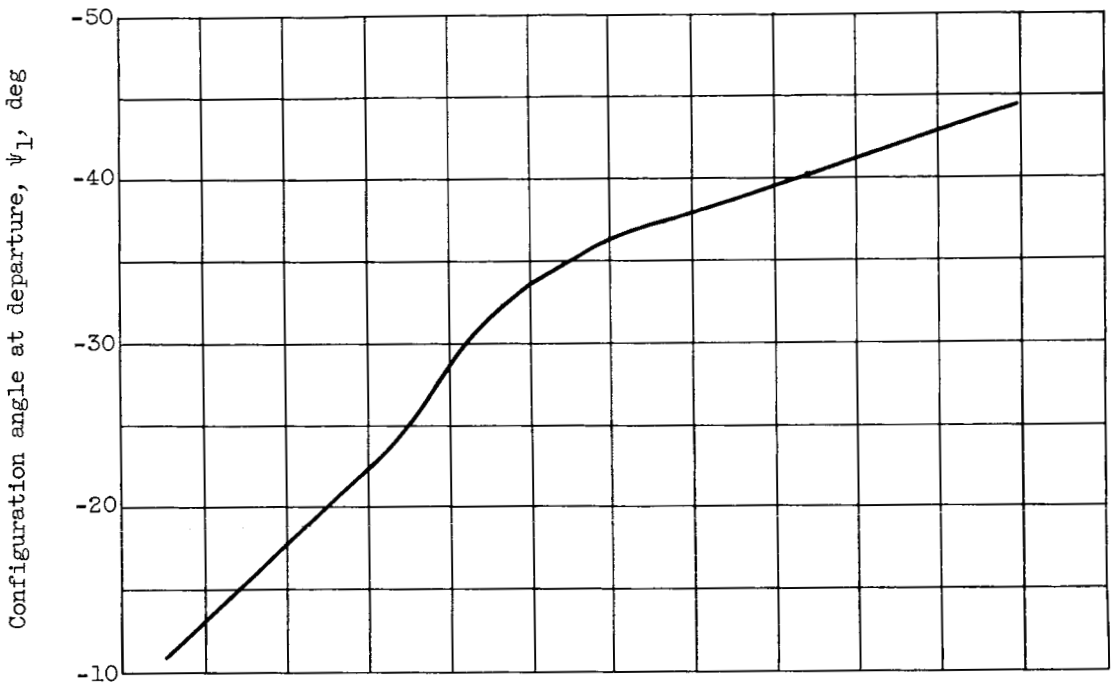


(d) Configuration angle at departure.

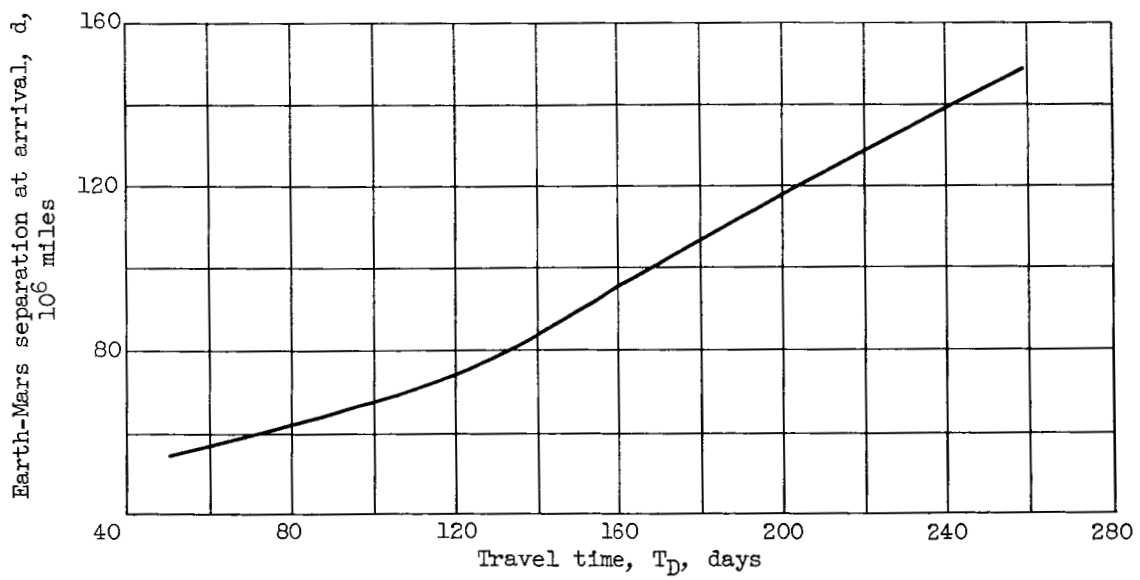


(e) Earth-Mars separation at arrival.

Figure 7. - Concluded. Path parameters for an orbiting Martian probe launched from an orbit of 1.1 Earth radii. Terminal orbit is at 1.1 Mars radii. Data for minimum sum of hyperbolic velocities at Earth's and Mars' orbits.

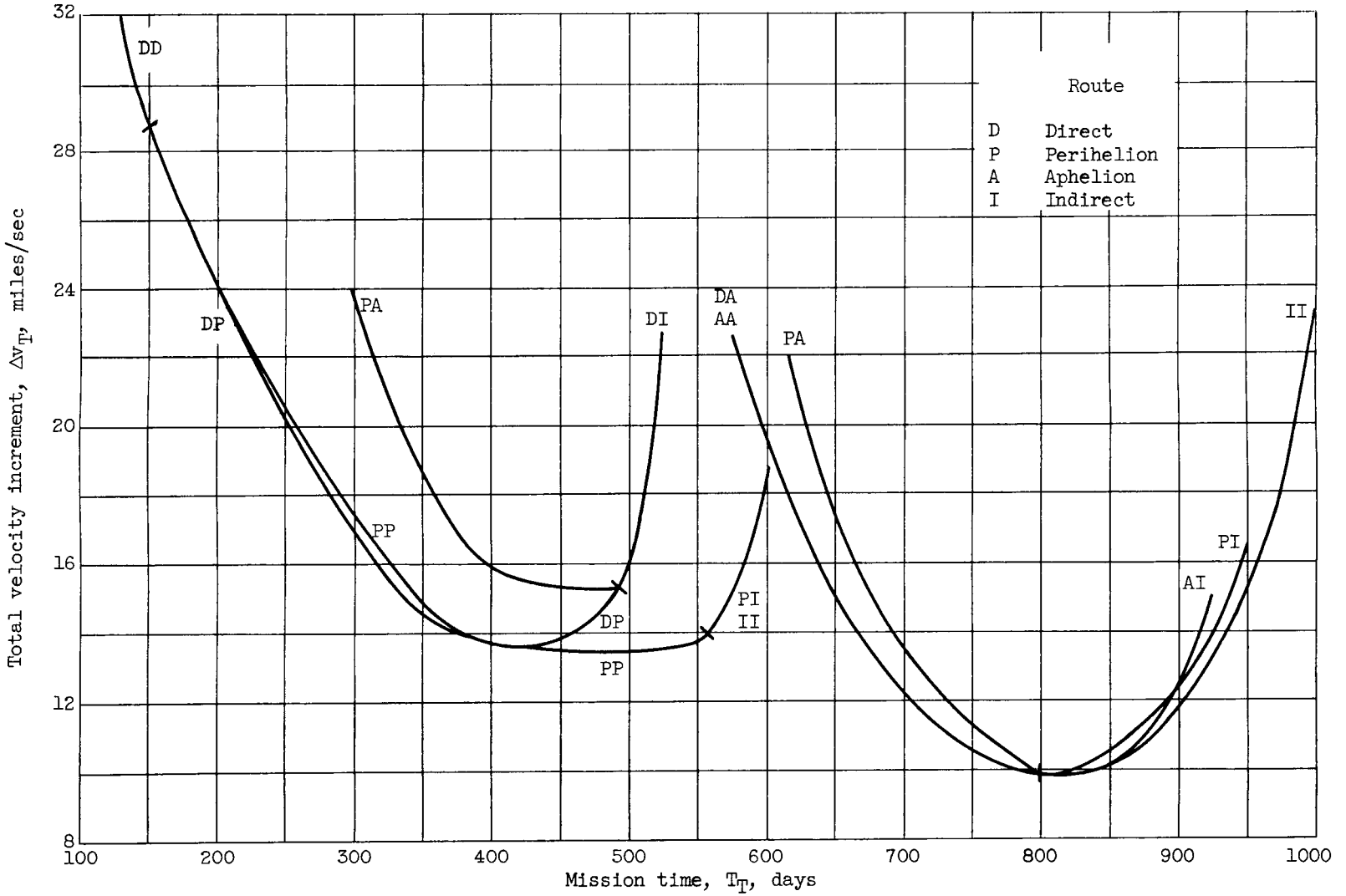


Figure 8. - Total velocity increments and mission times for round trips to Mars starting, waiting, and ending in circular orbits at 1.1 planet radii. Wait time, 0 days.

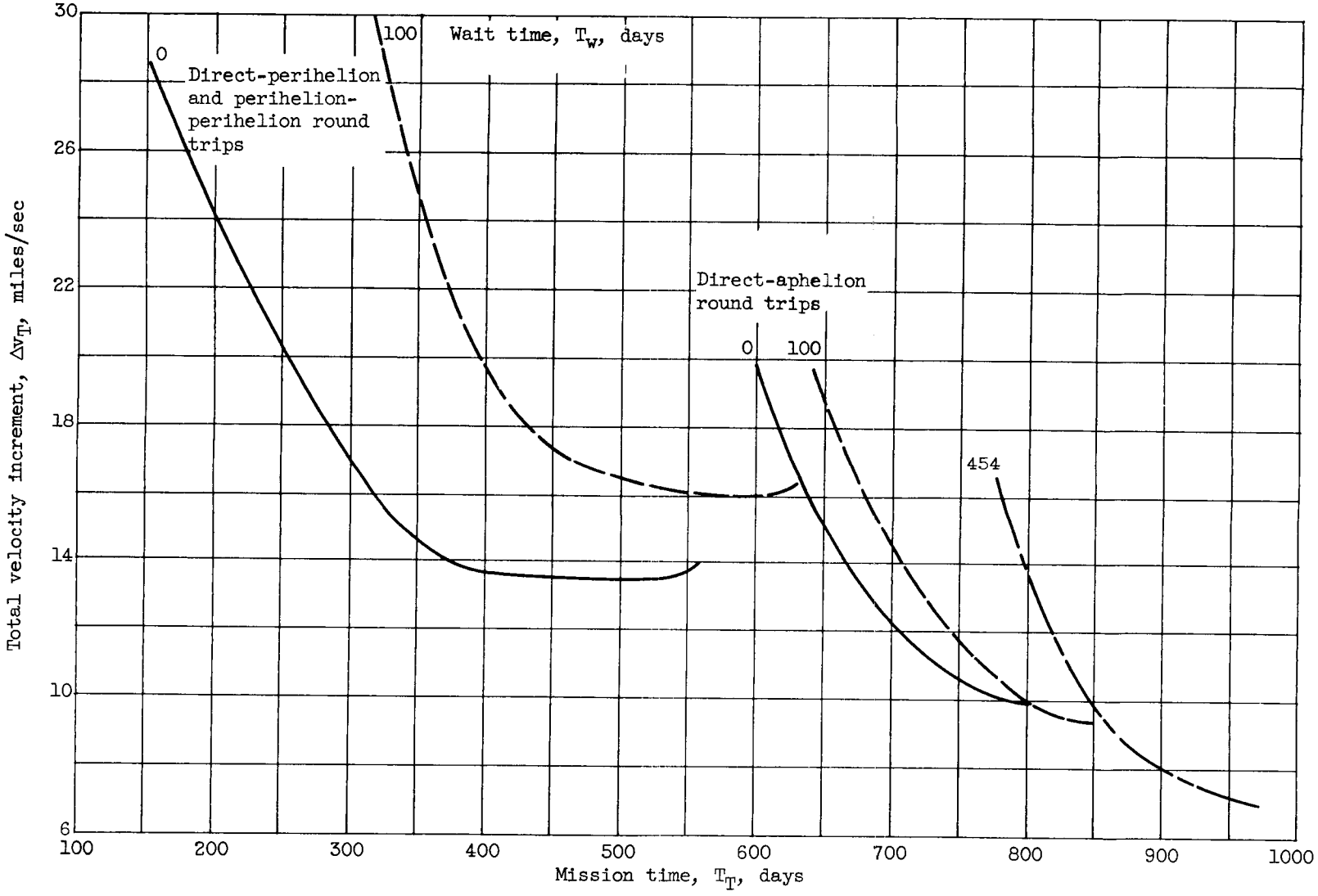


Figure 9. - Effect of wait time at Mars on total velocity increment and mission time for round trips to Mars starting, waiting, and ending in circular orbits at 1.1 planet radii.

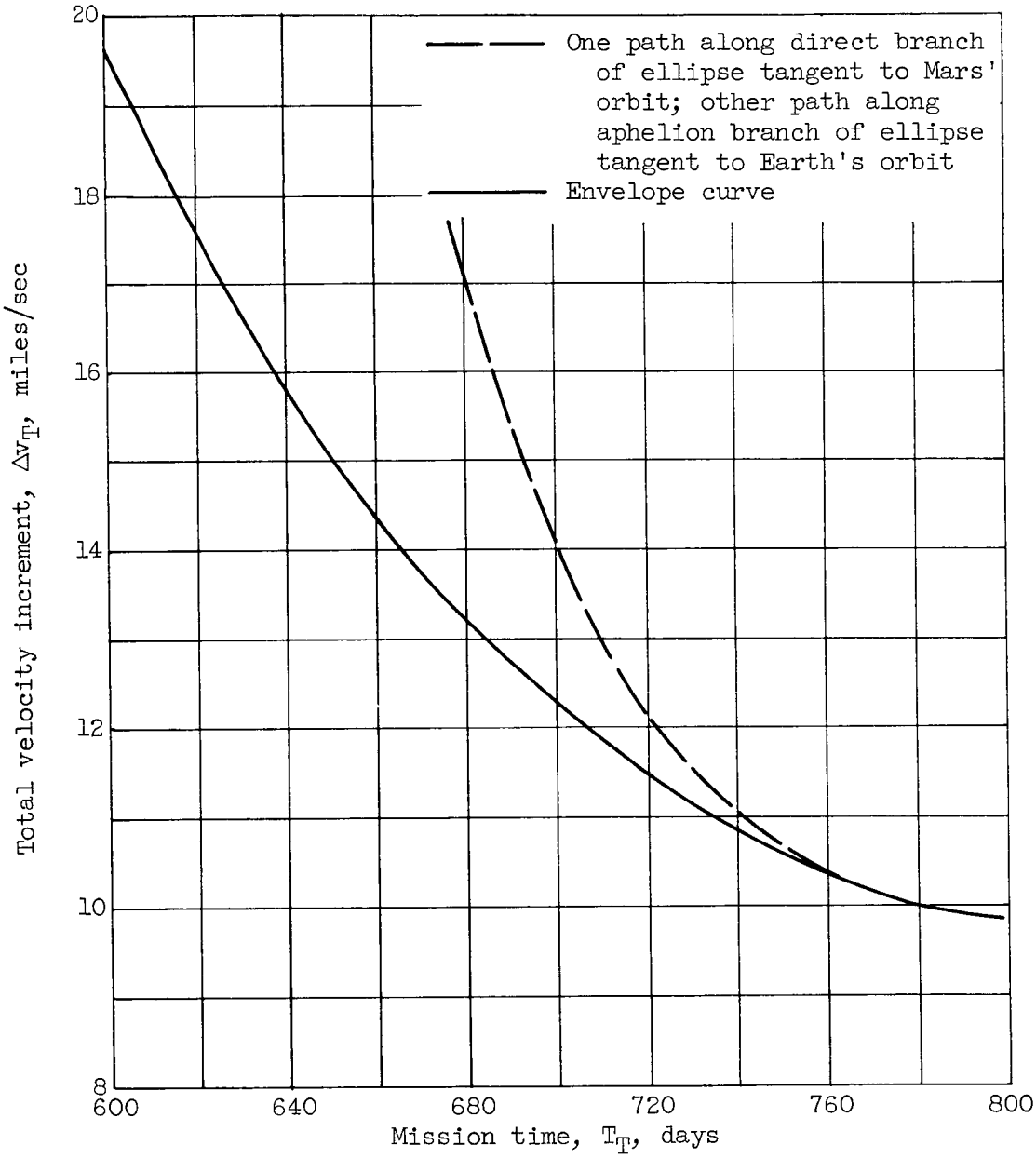


(a) Wait time in parking orbit at Mars, 0 days.

Figure 10. - Velocity increments and mission times for direct-aphelion round trips to Mars starting, waiting, and ending in circular orbits at 1.1 planet radii.

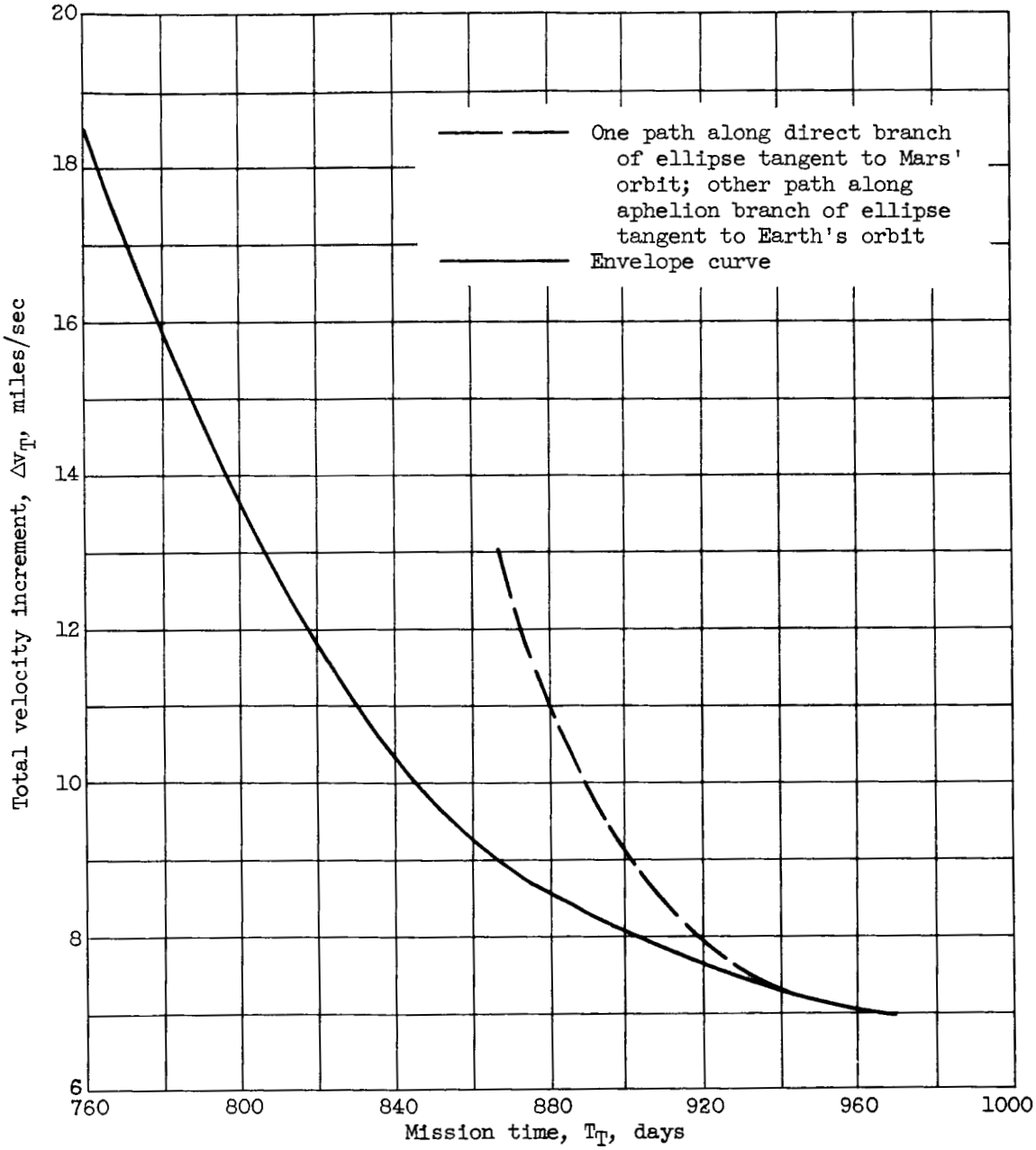


(b) Wait time in parking orbit at Mars, 454 days.

Figure 10. - Concluded. Velocity increments and mission times for direct-aphelion round trips to Mars starting, waiting, and ending in circular orbits at 1.1 planet radii.

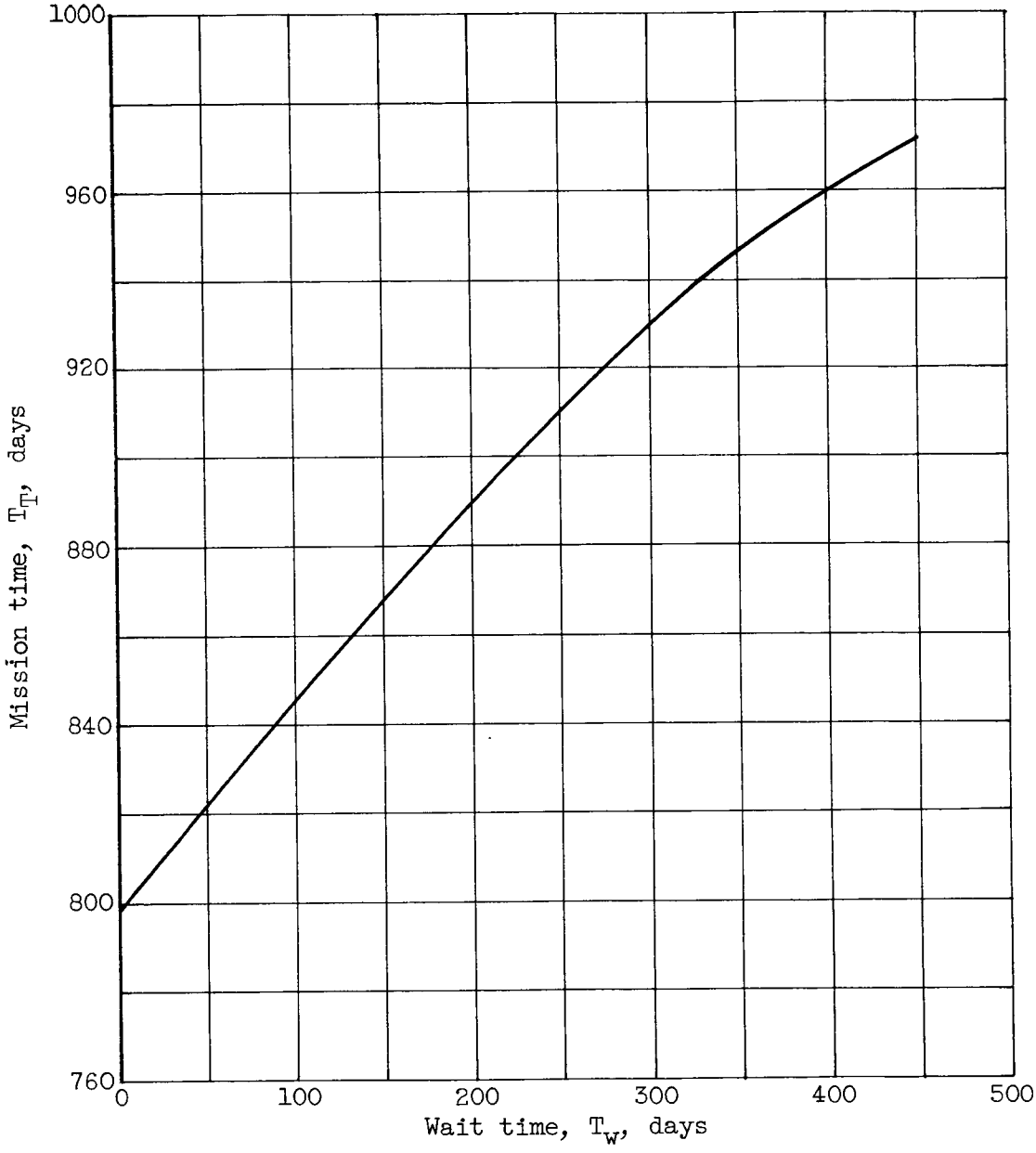


(a) Mission time.

Figure 11. - Path parameters for direct-aphelion round trips to Mars starting, waiting, and ending in circular orbits at 1.1 planet radii. One path along Hohmann ellipse; other path along aphelion branch of ellipse tangent to Earth's orbit. Data for minimum total velocity increment.

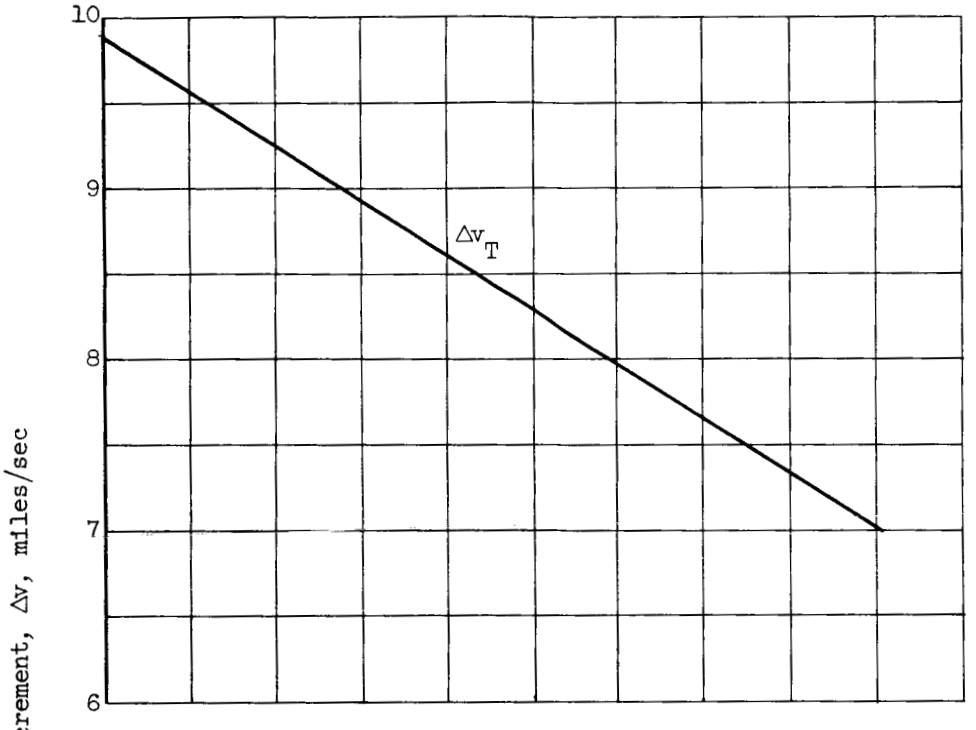


(b) Total velocity increment.

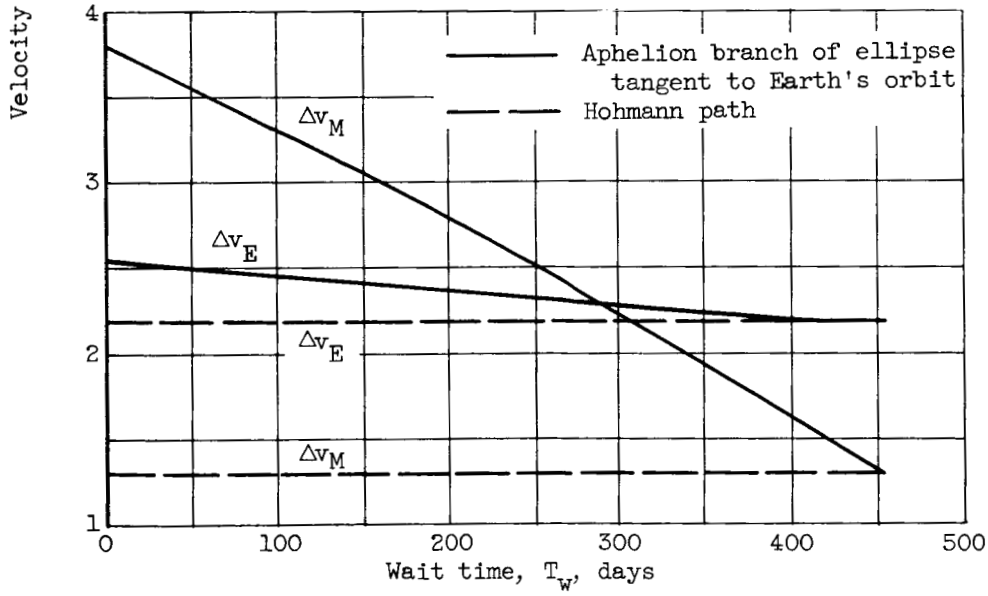


(c) Velocity increments at Earth and Mars.

Figure 11. - Continued. Path parameters for direct-aphelion round trips to Mars starting, waiting, and ending in circular orbits at 1.1 planet radii. One path along Hohmann ellipse; other path along aphelion branch of ellipse tangent to Earth's orbit. Data for minimum total velocity increment.

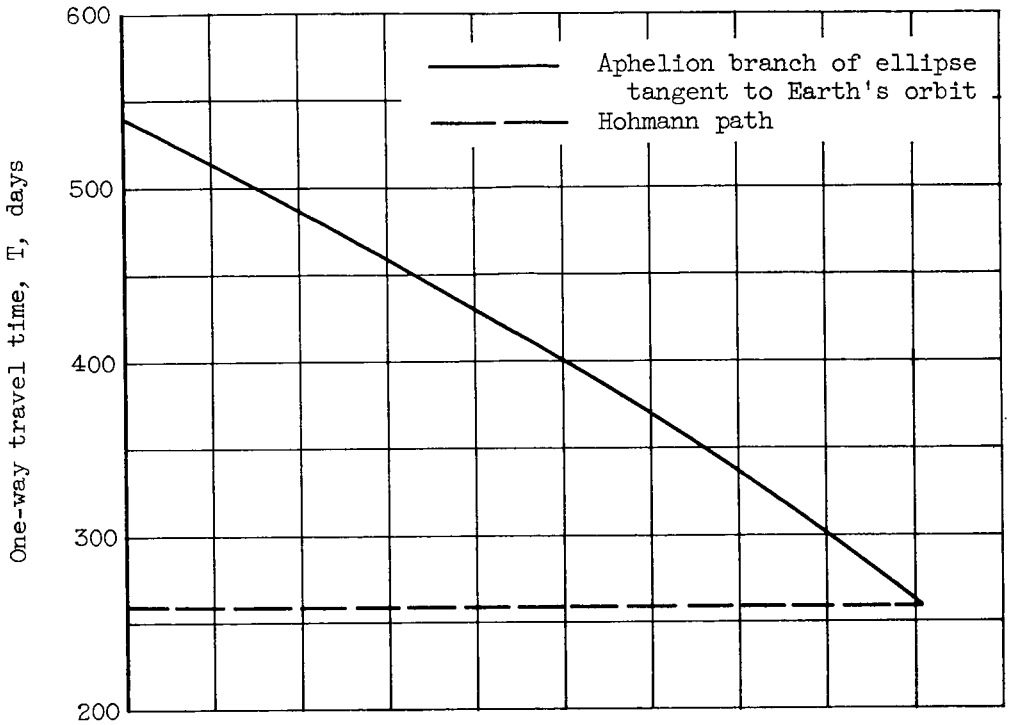


(d) One-way travel time.

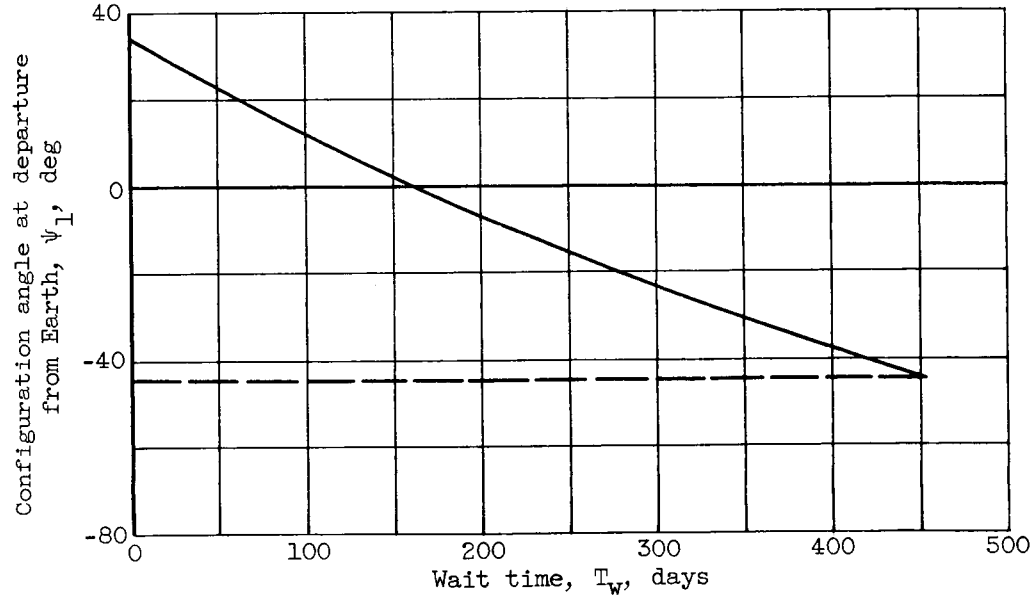


(e) Configuration angle at departure from Earth.

Figure 11. - Concluded. Path parameters for direct-aphelion round trips to Mars starting, waiting, and ending in circular orbits at 1.1 planet radii. One path along Hohmann ellipse; other path along aphelion branch of ellipse tangent to Earth's orbit. Data for minimum total velocity increment.

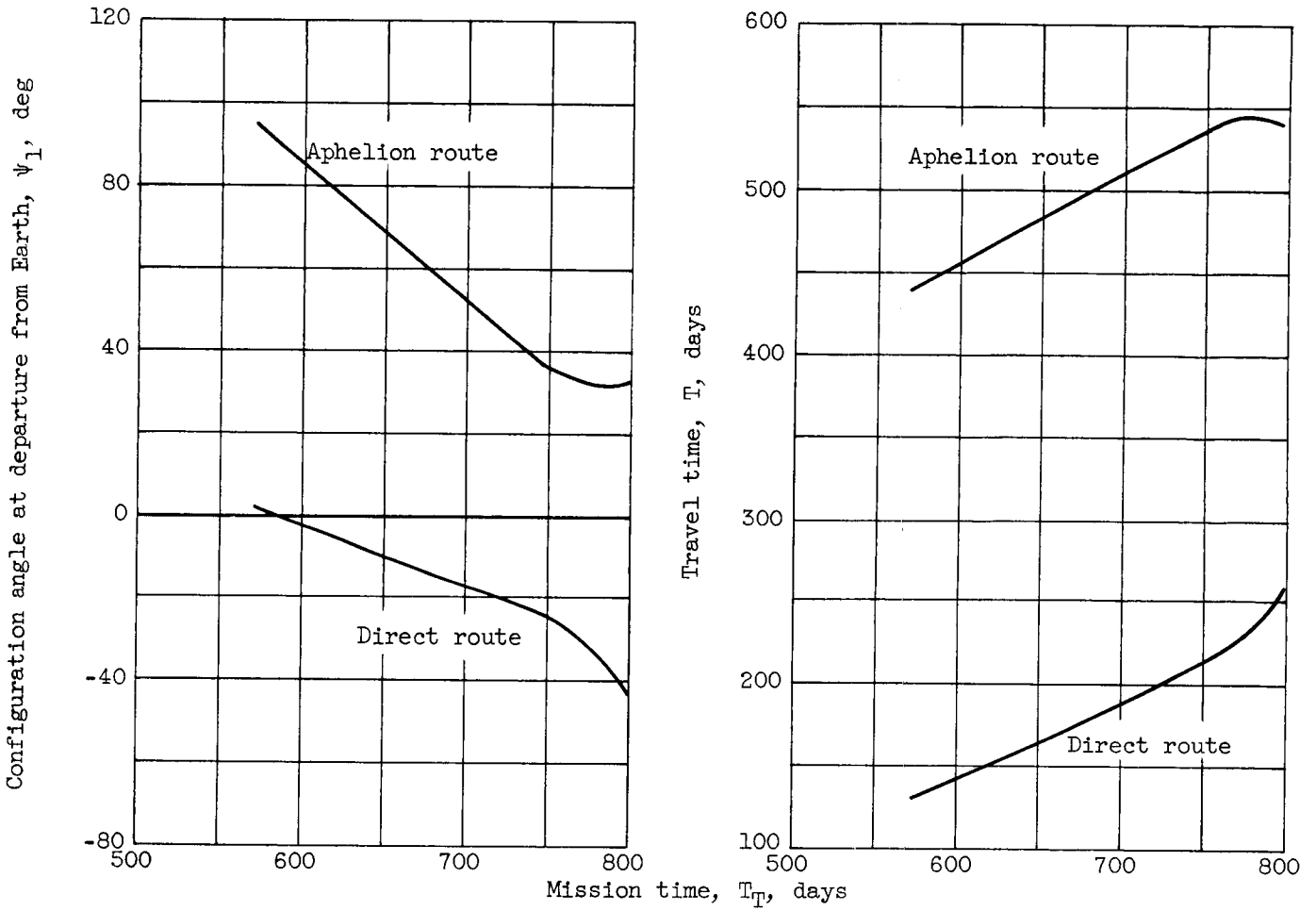


(a) Configuration angle at departure from Earth.

(b) Travel time.

Figure 12. - Path parameters for direct-aphelion round trips to Mars starting, waiting, and ending in circular orbits at 1.1 planet radii. Wait time in parking orbit at Mars, 0 days.

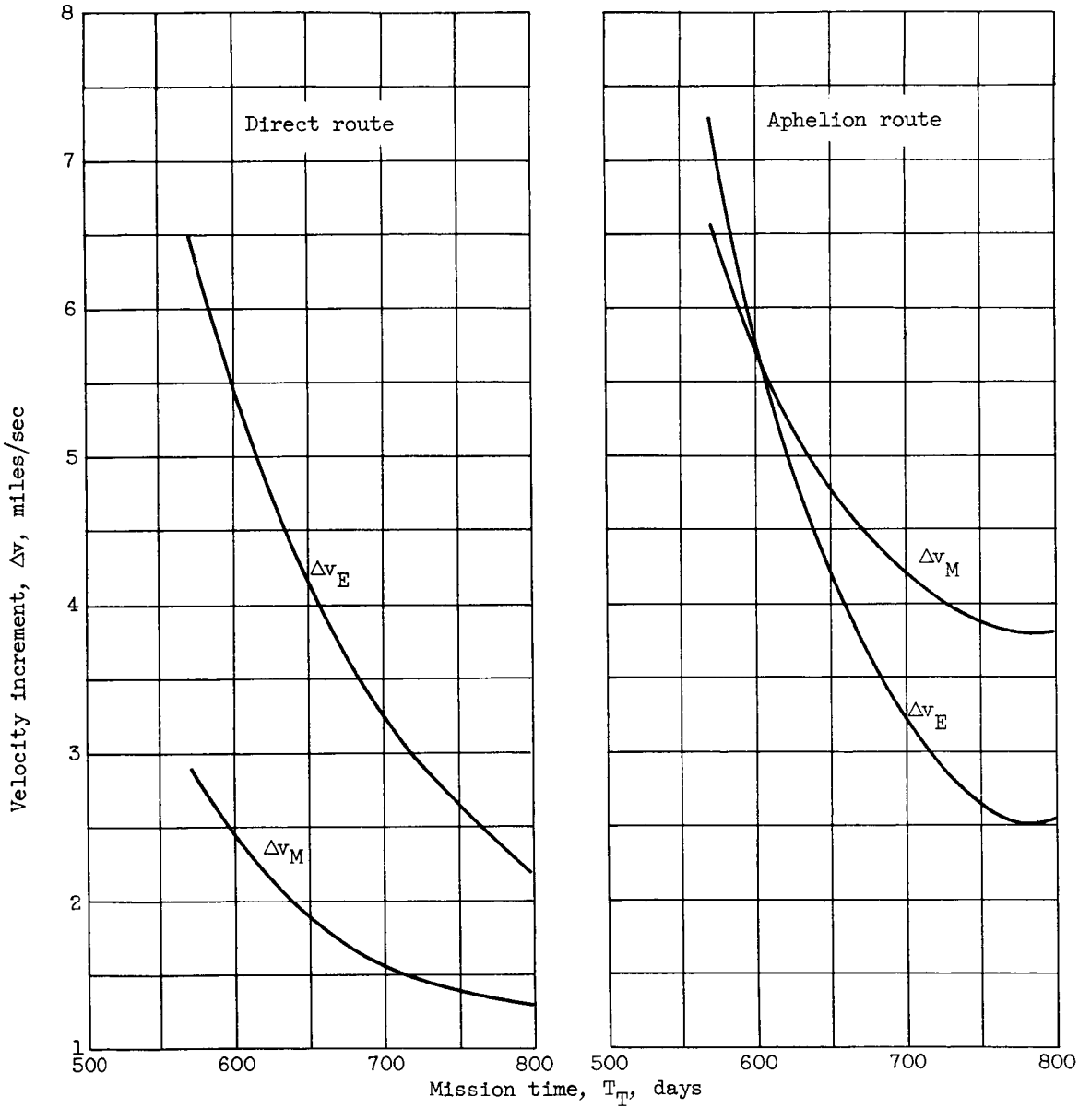


(c) Velocity increments at Earth and Mars.

Figure 12. - Concluded. Path parameters for direct-aphelion round trips to Mars starting, waiting, and ending in circular orbits at 1.1 planet radii. Wait time in parking orbit at Mars, 0 days.

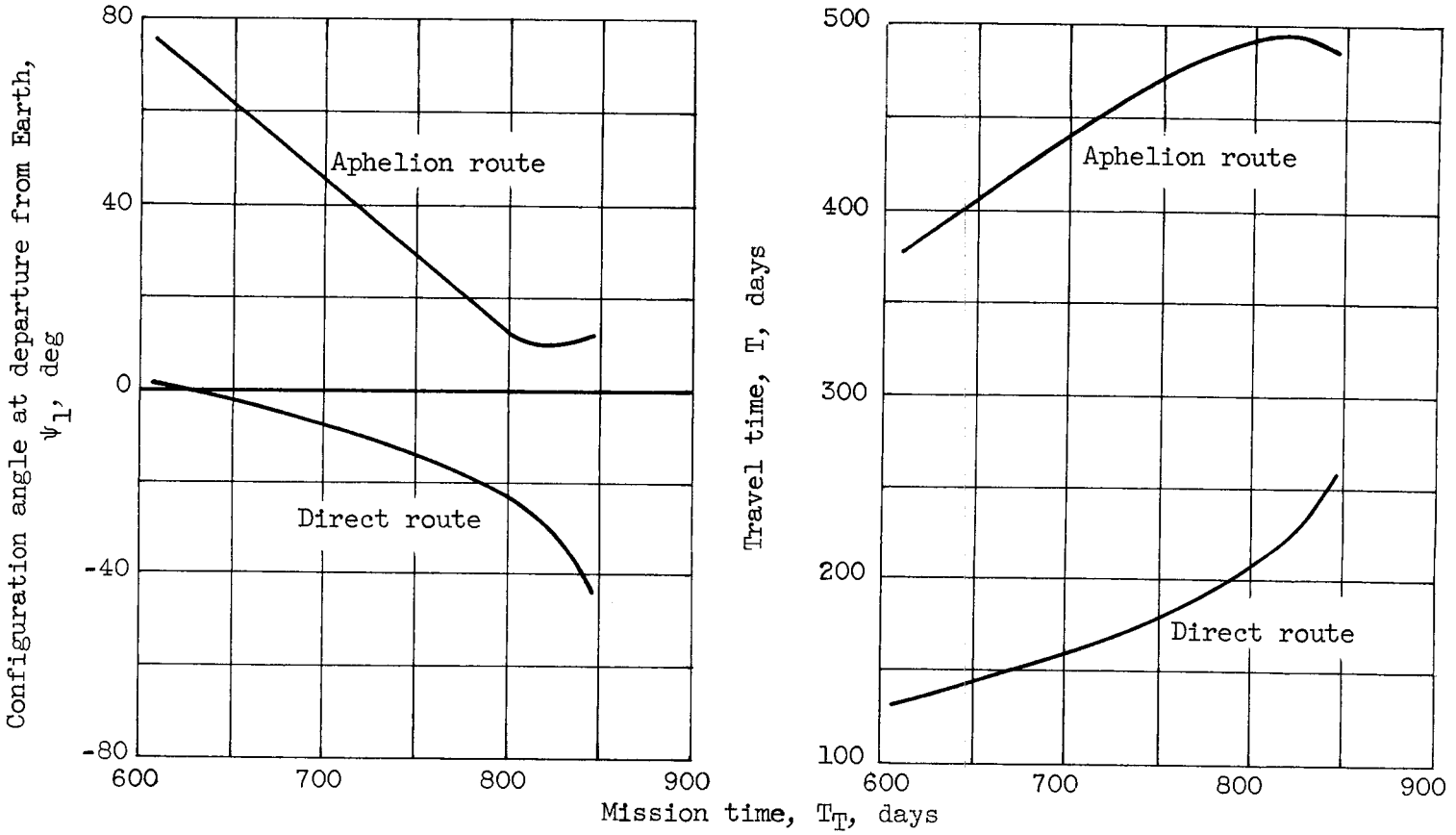


(a) Configuration angle at departure from Earth.

(b) Travel time.

Figure 13. - Path parameters for direct-aphelion round trips to Mars starting, waiting, and ending in circular orbits at 1.1 planet radii. Wait time in parking orbit at Mars, 100 days.

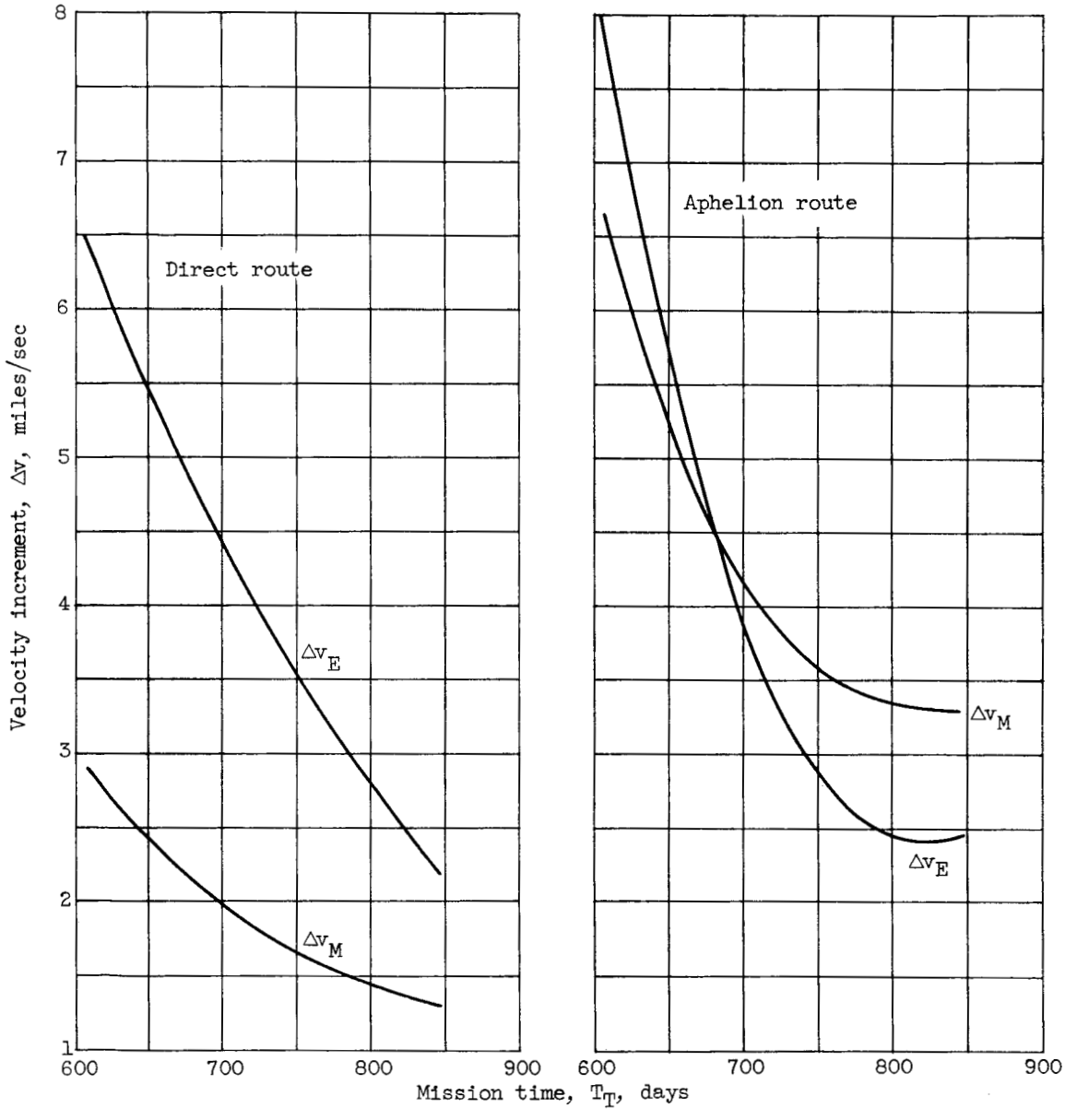


(c) Velocity increments at Earth and Mars.

Figure 13. - Concluded. Path parameters for direct-aphelion round trips to Mars starting, waiting, and ending in circular orbits at 1.1 planet radii. Wait time in parking orbit at Mars, 100 days.

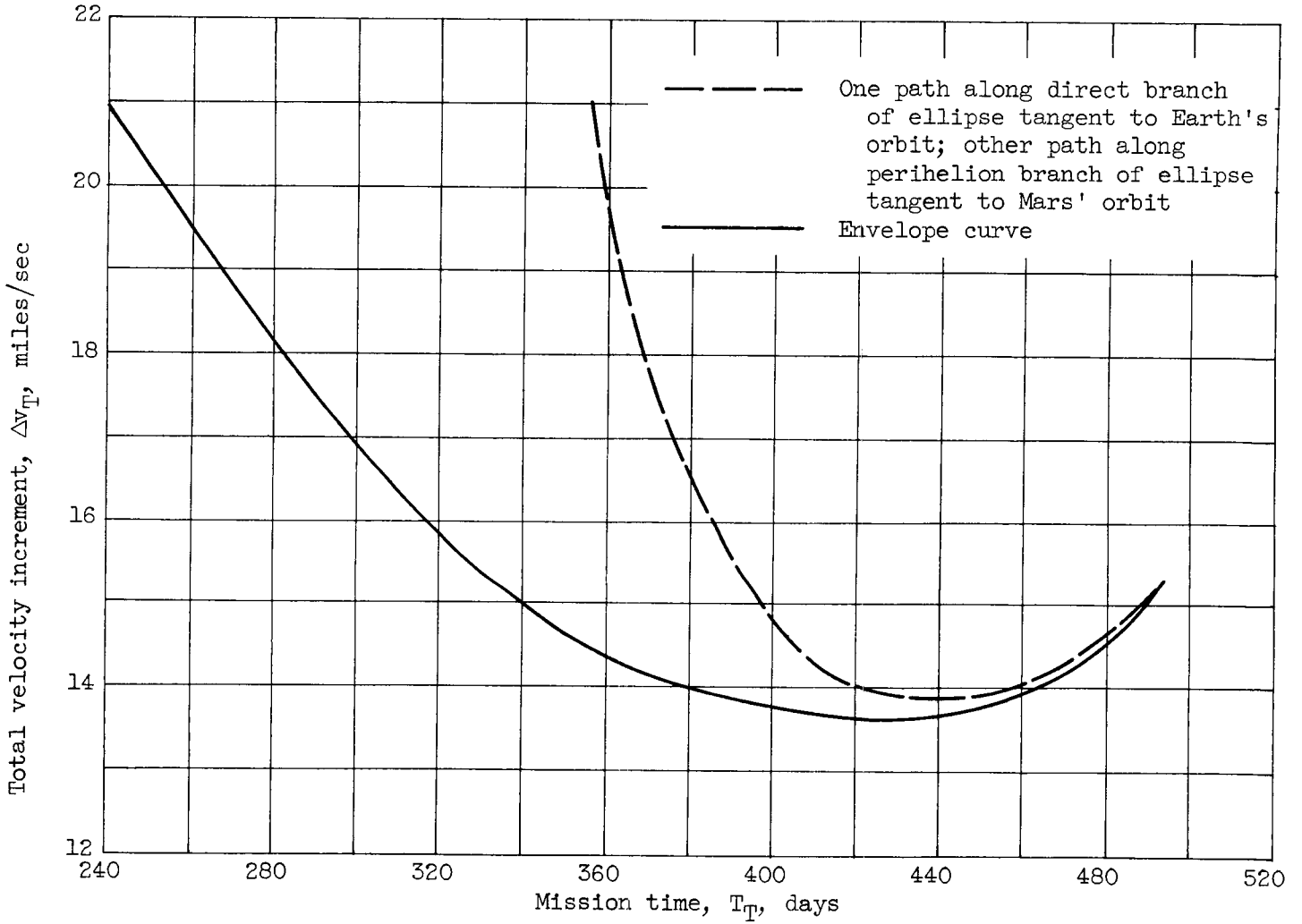


(a) Wait time in parking orbit at Mars, 0 days.

Figure 14. - Velocity increments and mission times for direct-perihelion round trips to Mars starting, waiting, and ending in circular orbits at 1.1 planet radii.

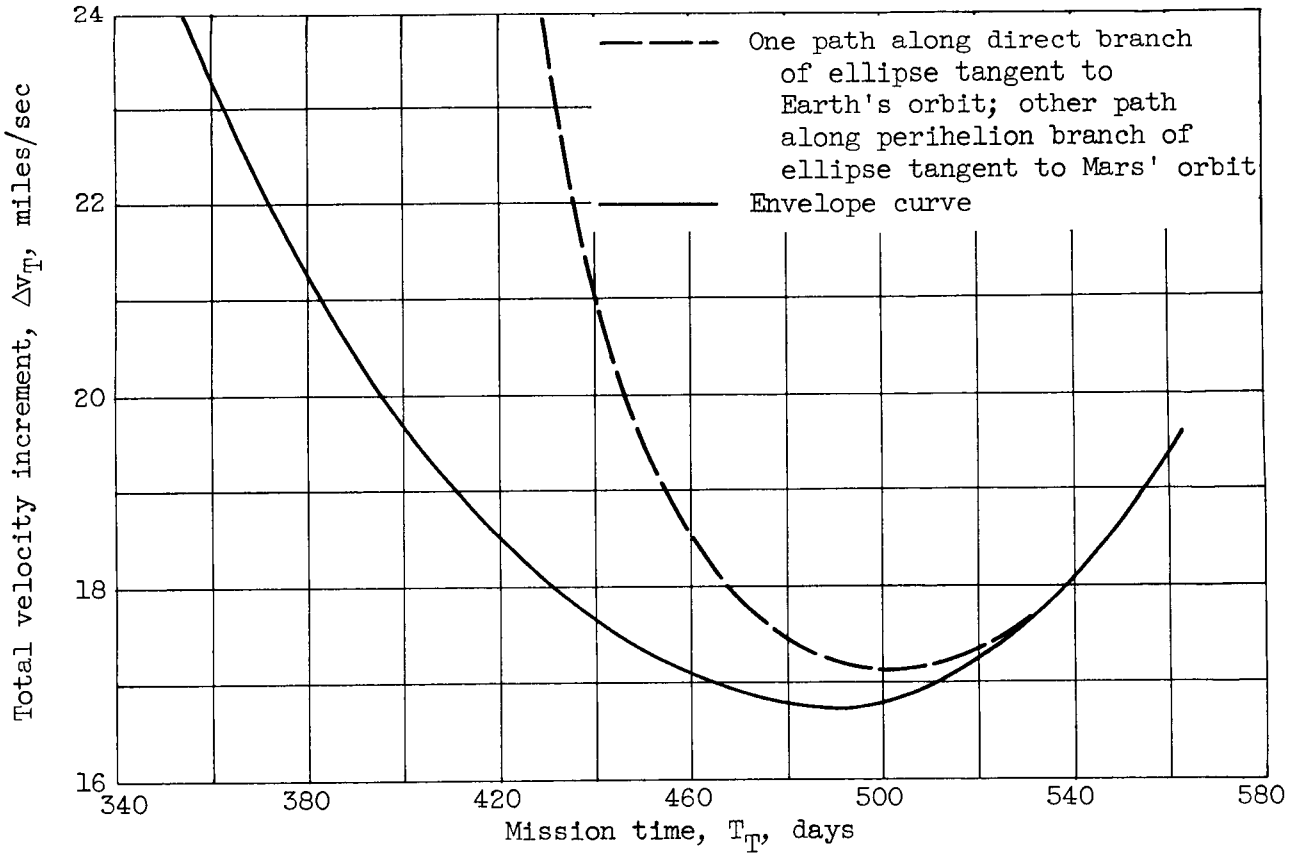


(b) Wait time in parking orbit at Mars, 100 days.

Figure 14. - Concluded. Velocity increments and mission times for direct-perihelion round trips to Mars starting, waiting, and ending in circular orbits at 1.1 planet radii.

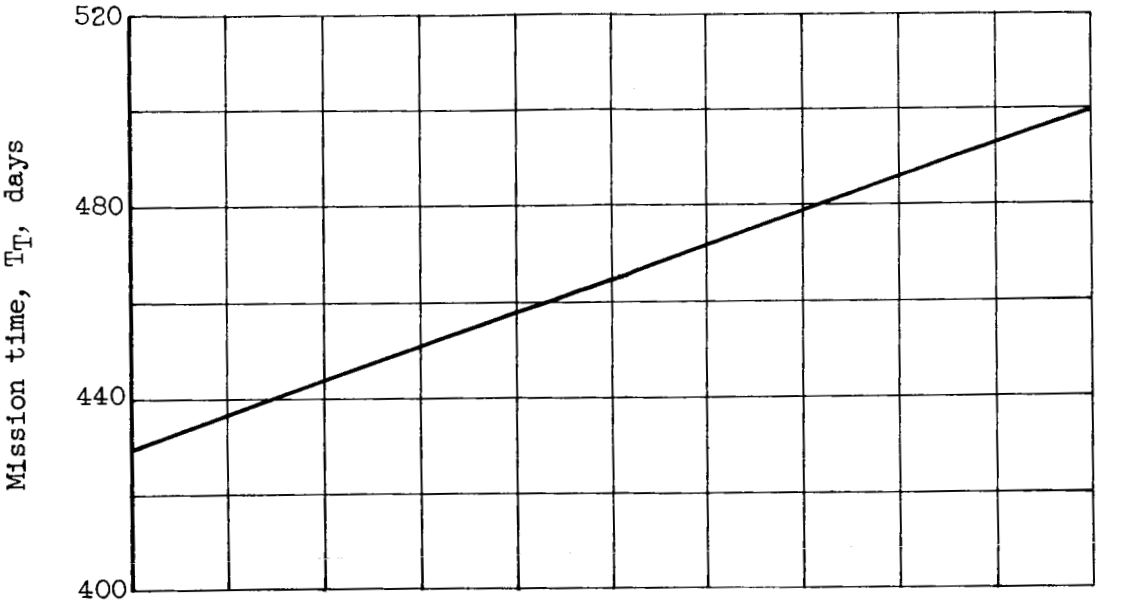


(a) Mission time.

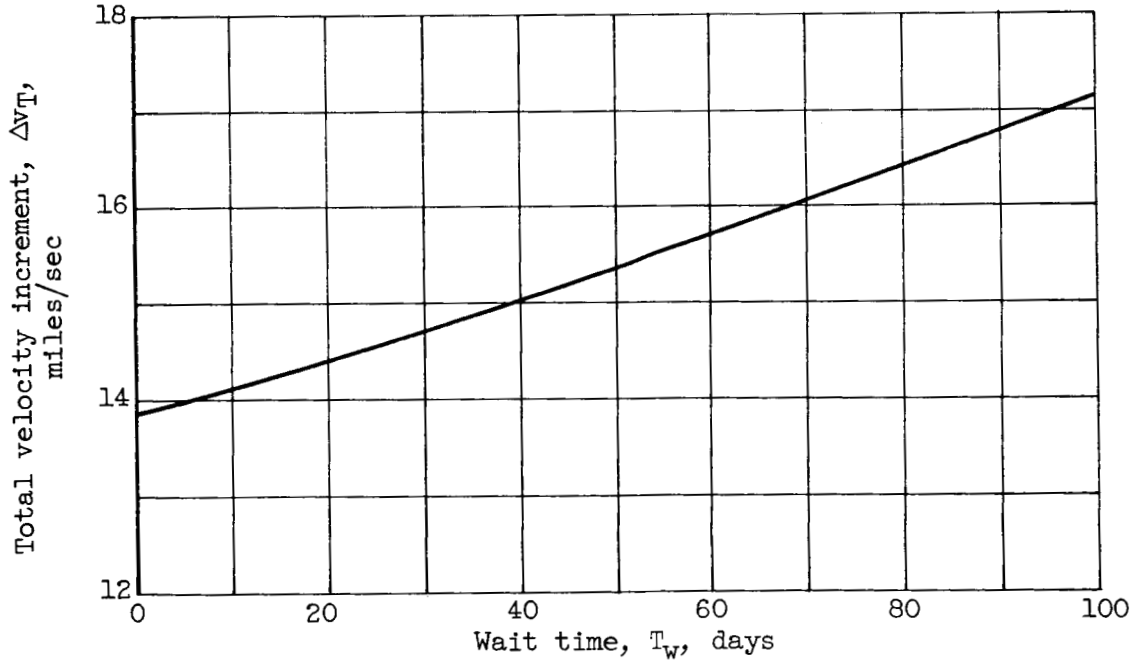


(b) Total velocity increment.

Figure 15. - Path parameters for direct-perihelion round trips to Mars starting, waiting, and ending in circular orbits at 1.1 planet radii. One path along direct branch of ellipse tangent to Earth's orbit and the other along the perihelion branch of an ellipse tangent to Mars' orbit. Data for minimum total velocity increment.

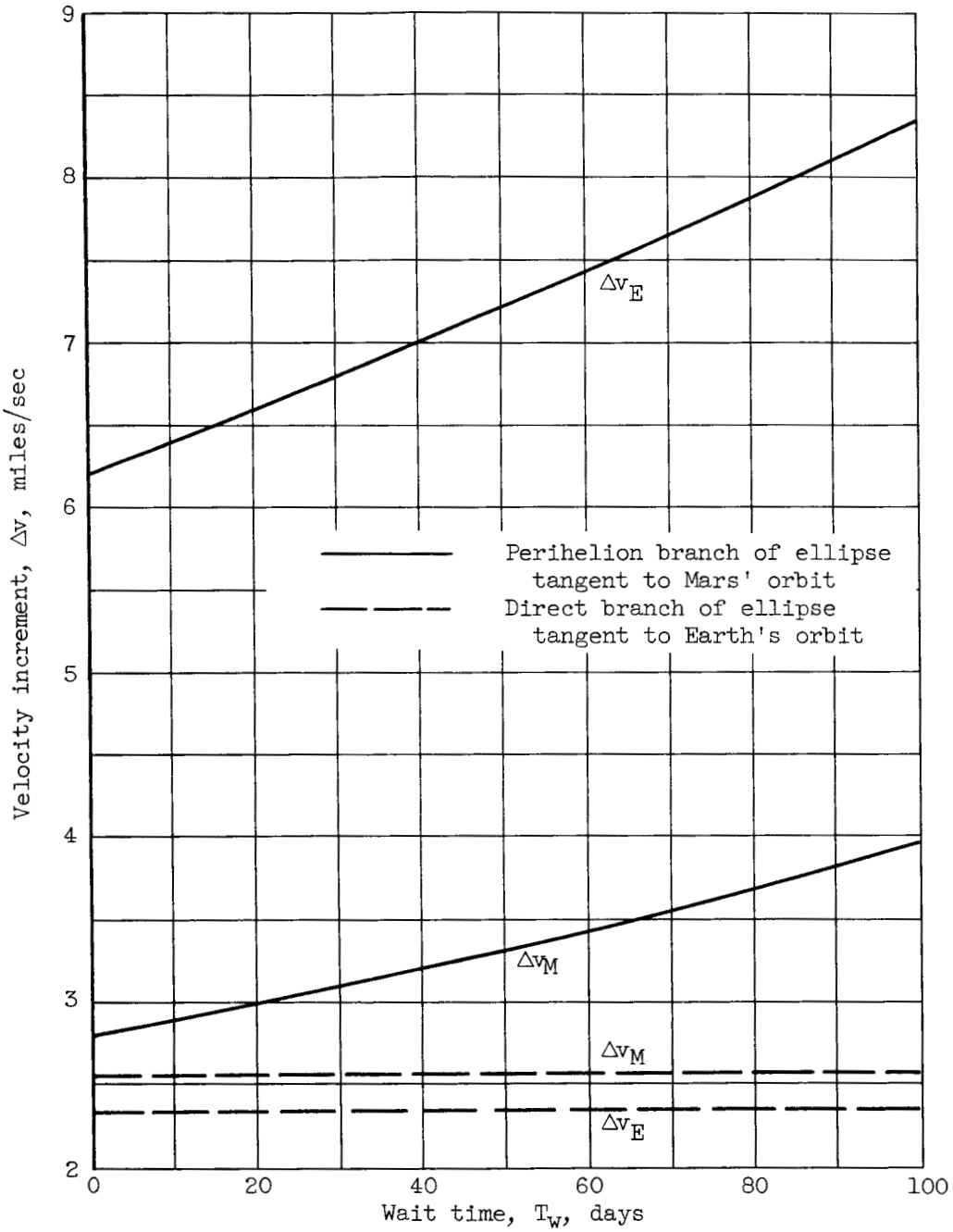


(c) Velocity increments at Earth and Mars.

Figure 15. - Continued. Path parameters for direct-perihelion round trips to Mars starting, waiting, and ending in circular orbits at 1.1 planet radii. One path along direct branch of ellipse tangent to Earth's orbit and the other along the perihelion branch of an ellipse tangent to Mars' orbit. Data for minimum total velocity increment.

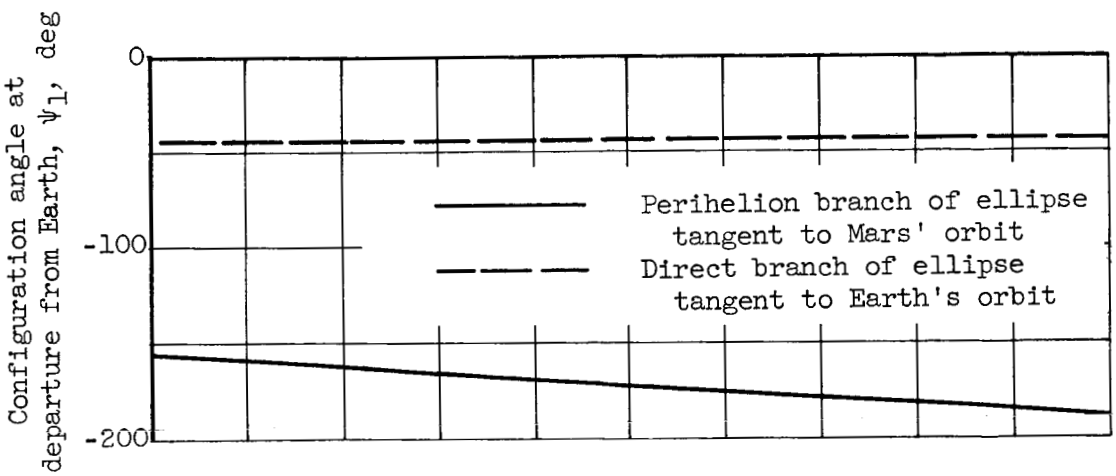


(d) Configuration angle at departure from Earth.

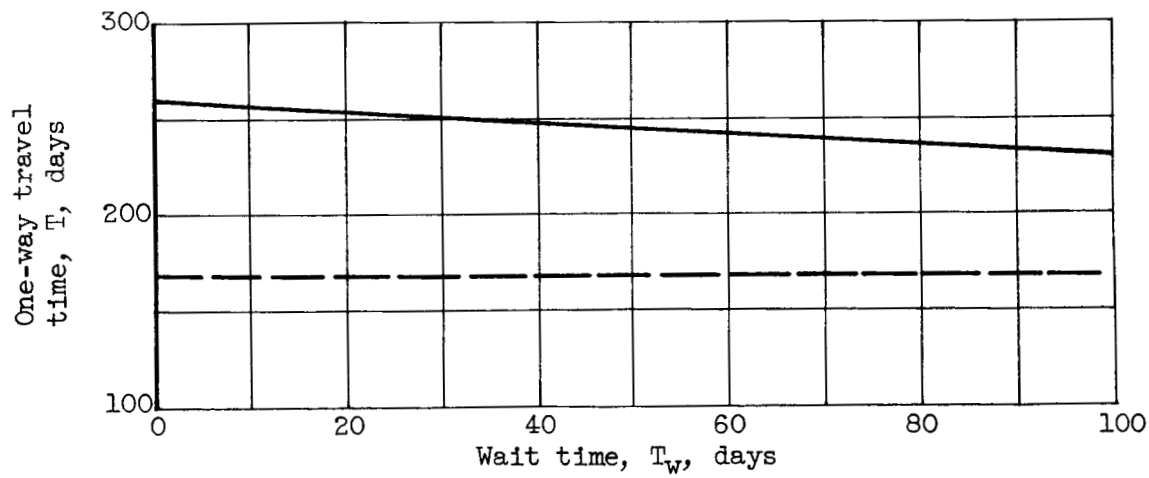


(e) One-way travel time.

Figure 15. - Concluded. Path parameters for direct-perihelion round trips to Mars starting, waiting, and ending in circular orbits at 1.1 planet radii. One path along direct branch of ellipse tangent to Earth's orbit and the other along the perihelion branch of an ellipse tangent to Mars' orbit. Data for minimum total velocity increment.

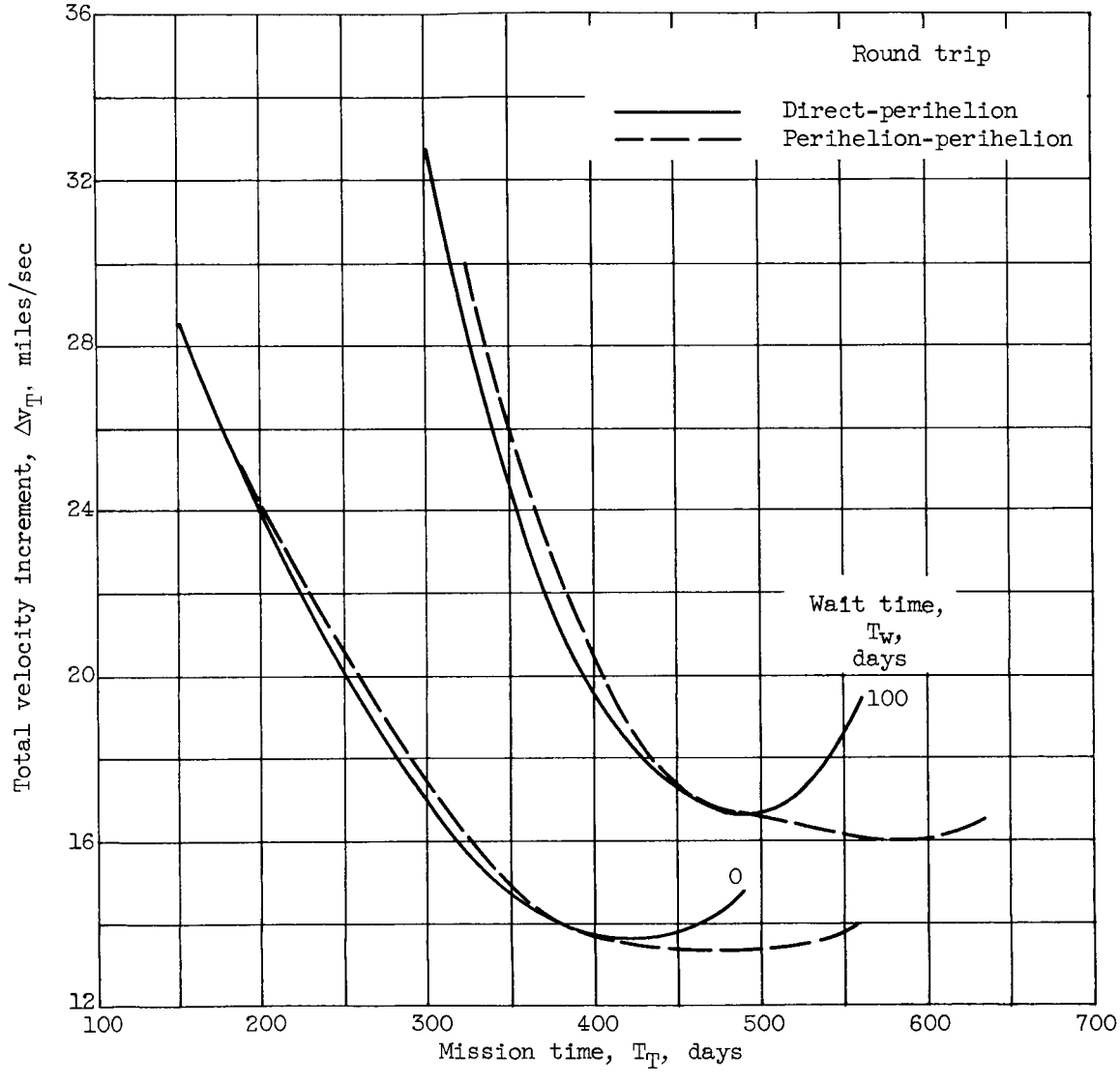


Figure 16. - Velocity increments and mission times for round trips to Mars starting, waiting, and ending in circular orbits at 1.1 planet radii. Direct-perihelion and perihelion-perihelion round trips.

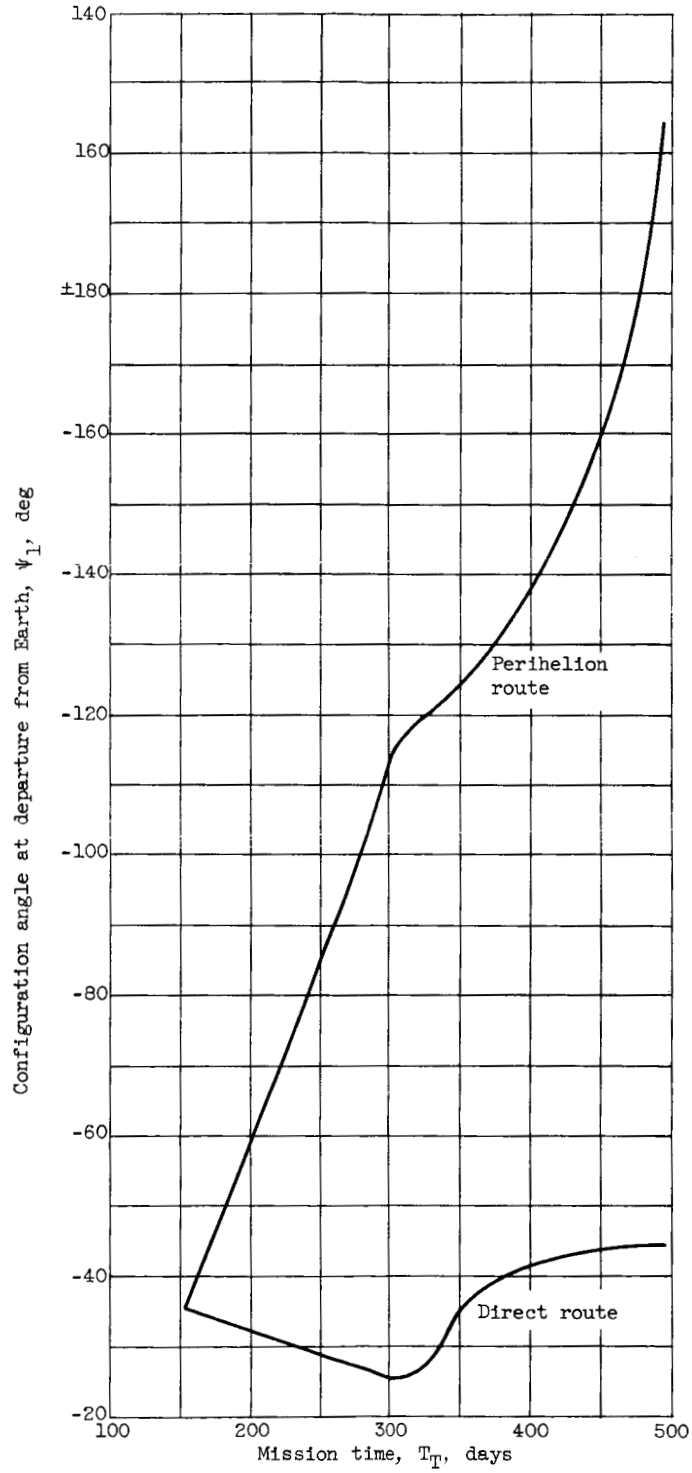


(a) Configuration angle at departure from Earth.

Figure 17. - Path parameters for direct-perihelion round trips to Mars starting, waiting, and ending in circular orbits at 1.1 planet radii. Wait time in parking orbit at Mars, 0 days.

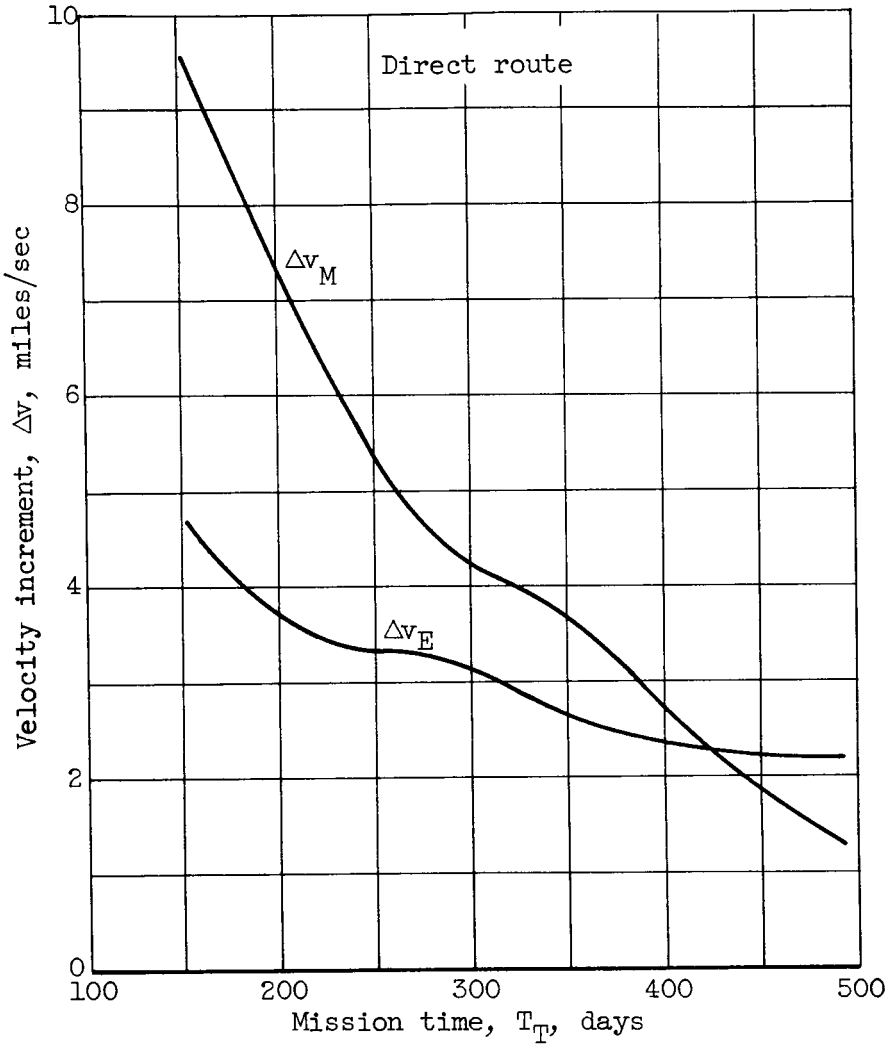


(b) Velocity increments at Earth and Mars for direct route.

Figure 17. - Continued. Path parameters for direct-perihelion round trips to Mars starting, waiting, and ending in circular orbits at 1.1 planet radii. Wait time in parking orbit at Mars, 0 days.

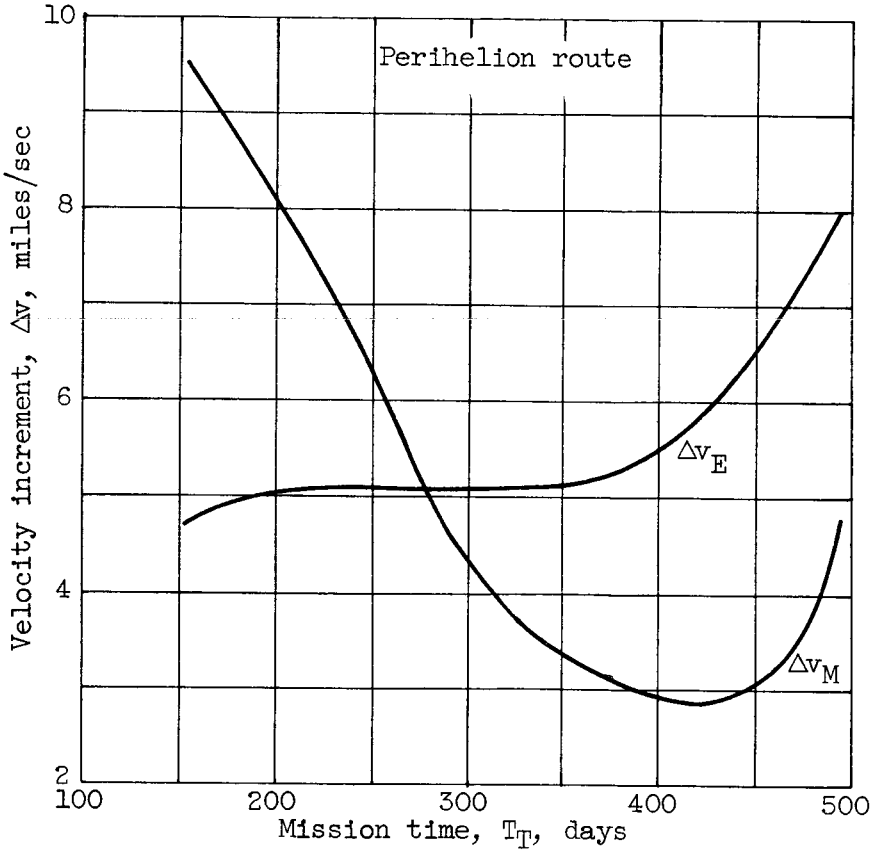


(c) Velocity increments at Earth and Mars for perihelion route.

Figure 17. - Continued. Path parameters for direct-perihelion round trips to Mars starting, waiting, and ending in circular orbits at 1.1 planet radii. Wait time in parking orbit at Mars, 0 days.

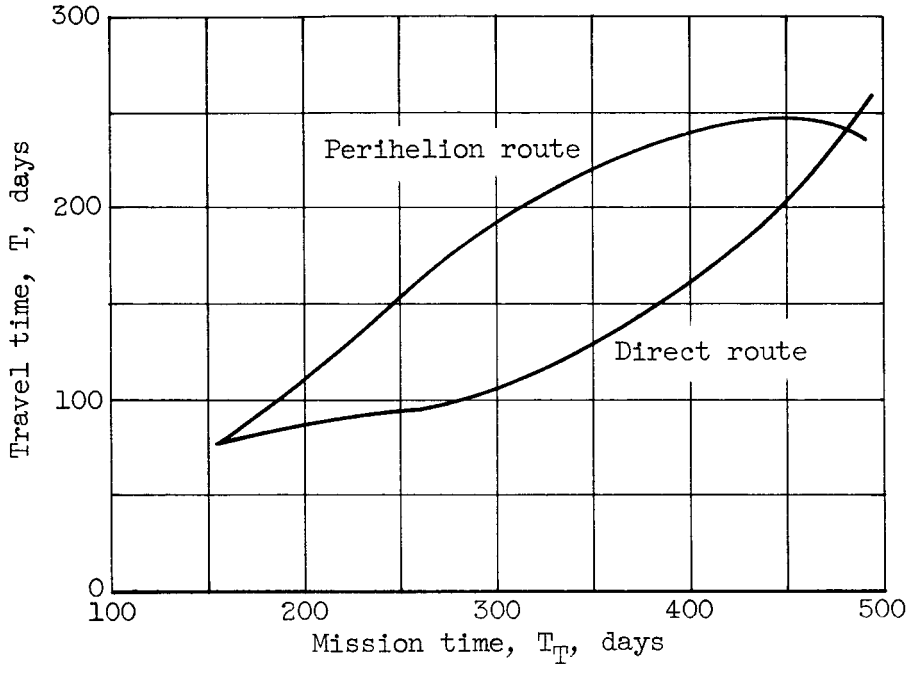


(d) Travel time.

Figure 17. - Concluded. Path parameters for direct-perihelion round trips to Mars starting, waiting, and ending in circular orbits at 1.1 planet radii. Wait time in parking orbit at Mars, 0 days.

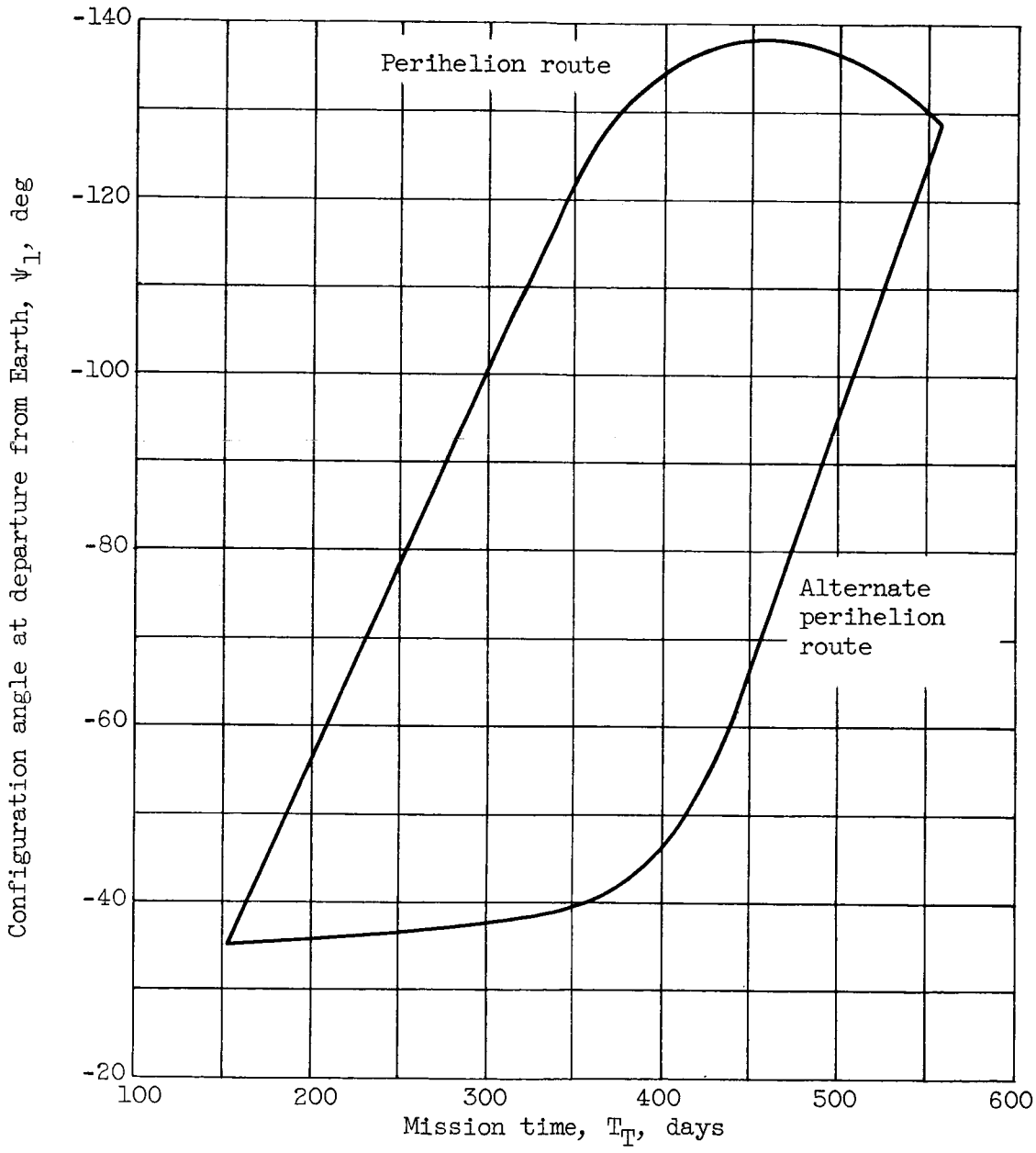


(a) Configuration angle at departure from Earth.

Figure 18. - Path parameters for perihelion-perihelion round trips to Mars starting, waiting, and ending in circular orbits at 1.1 planet radii. Wait time in parking orbit at Mars, 0 days.

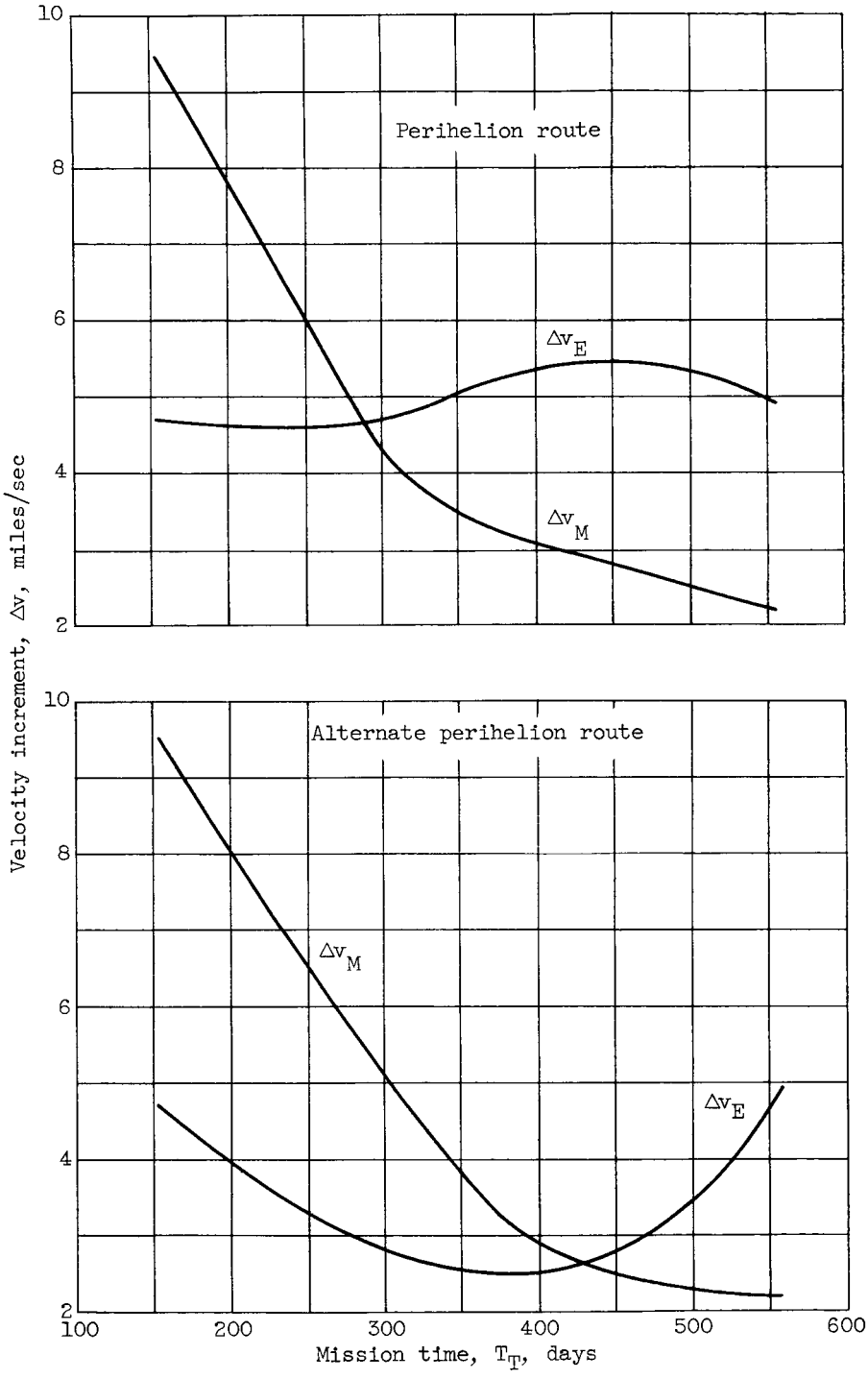


(b) Velocity increments at Earth and Mars.

Figure 18. - Continued. Path parameters for perihelion-perihelion round trips to Mars starting, waiting, and ending in circular orbits at 1.1 planet radii. Wait time in parking orbit at Mars, 0 days.

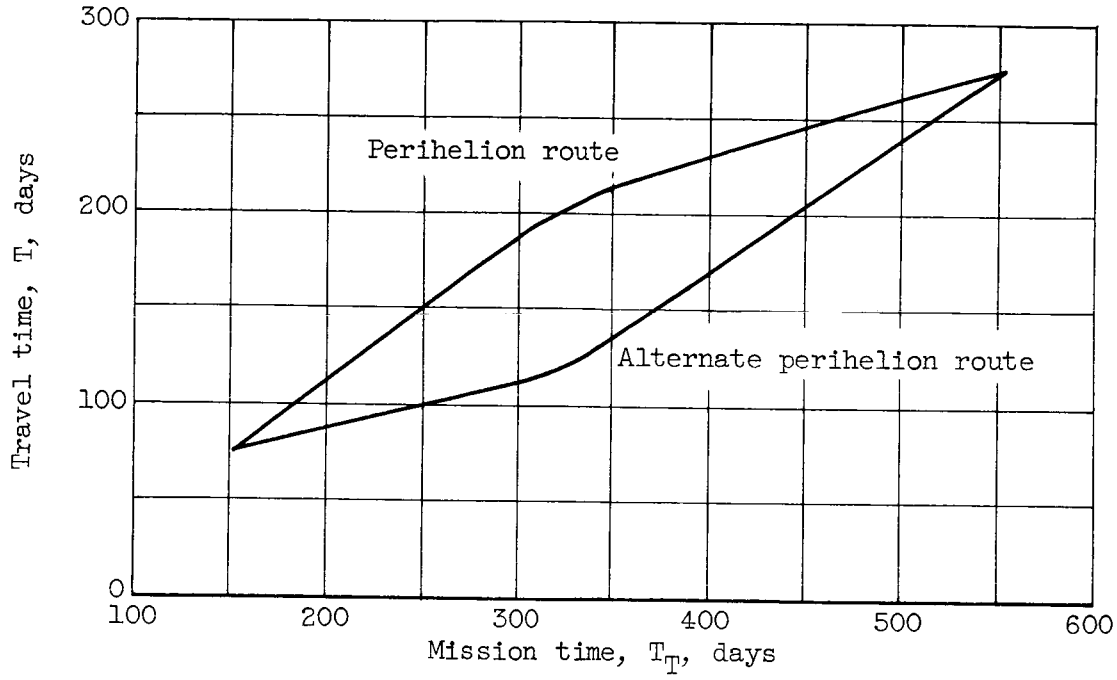


(c) Travel time.

Figure 18. - Concluded. Path parameters for perihelion-perihelion round trips to Mars starting, waiting, and ending in circular orbits at 1.1 planet radii. Wait time in parking orbit at Mars, 0 days.

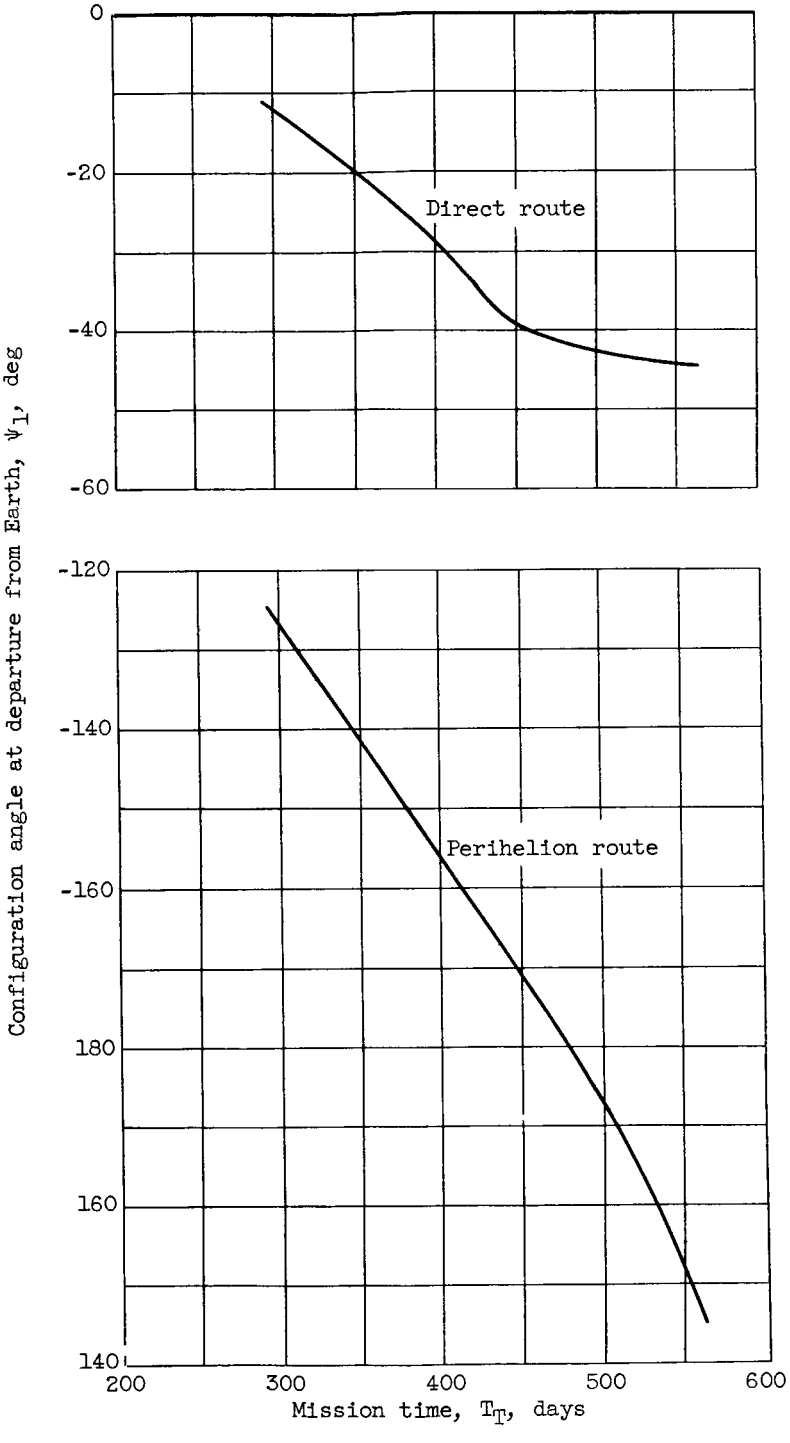


(a) Configuration angle at departure from Earth.

Figure 19. - Path parameters for direct-perihelion round trips to Mars starting, waiting, and ending in circular orbits at 1.1 planet radii. Wait time in parking orbit at Mars, 100 days.

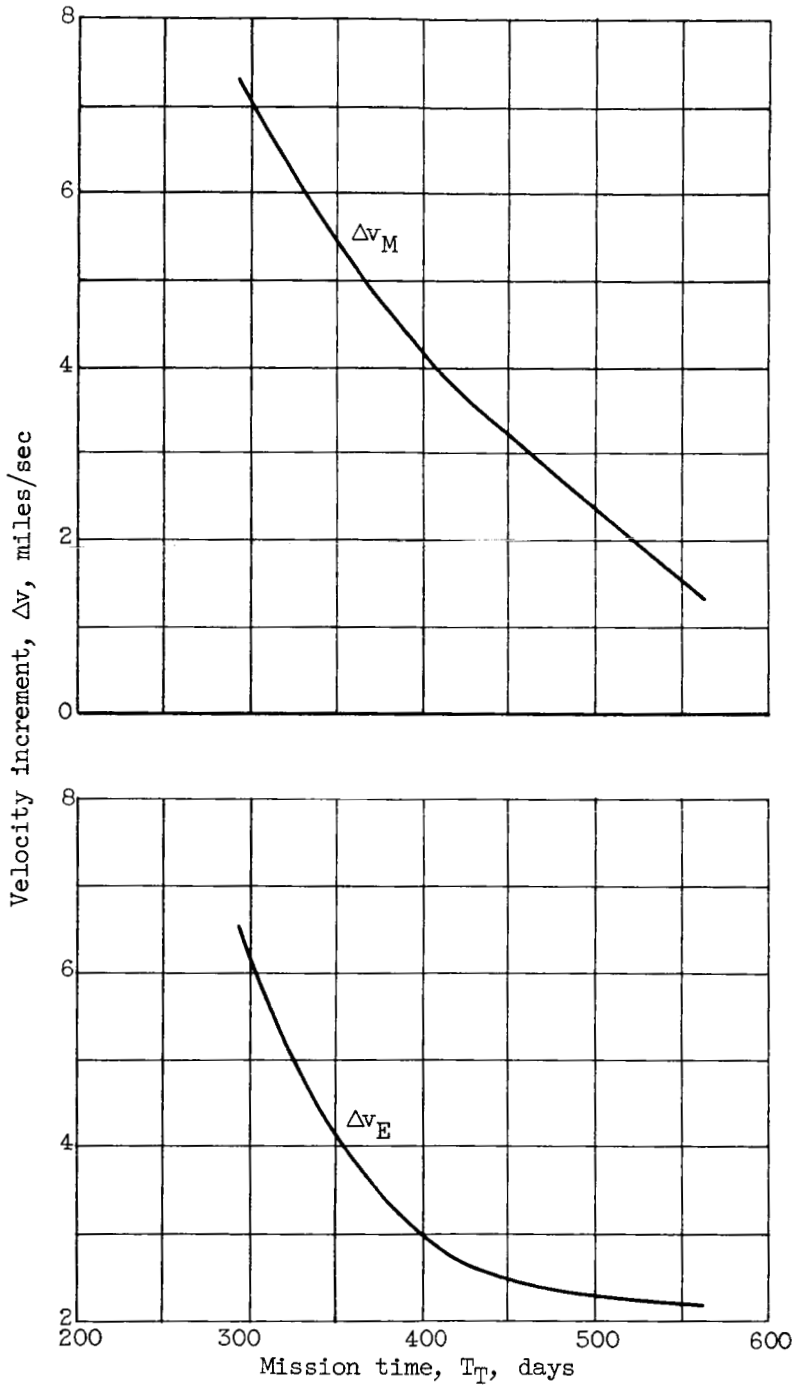


(b) Velocity increments at Earth and Mars for direct route.

Figure 19. - Continued. Path parameters for direct-perihelion round trips to Mars starting, waiting, and ending in circular orbits at 1.1 planet radii. Wait time in parking orbit at Mars, 100 days.

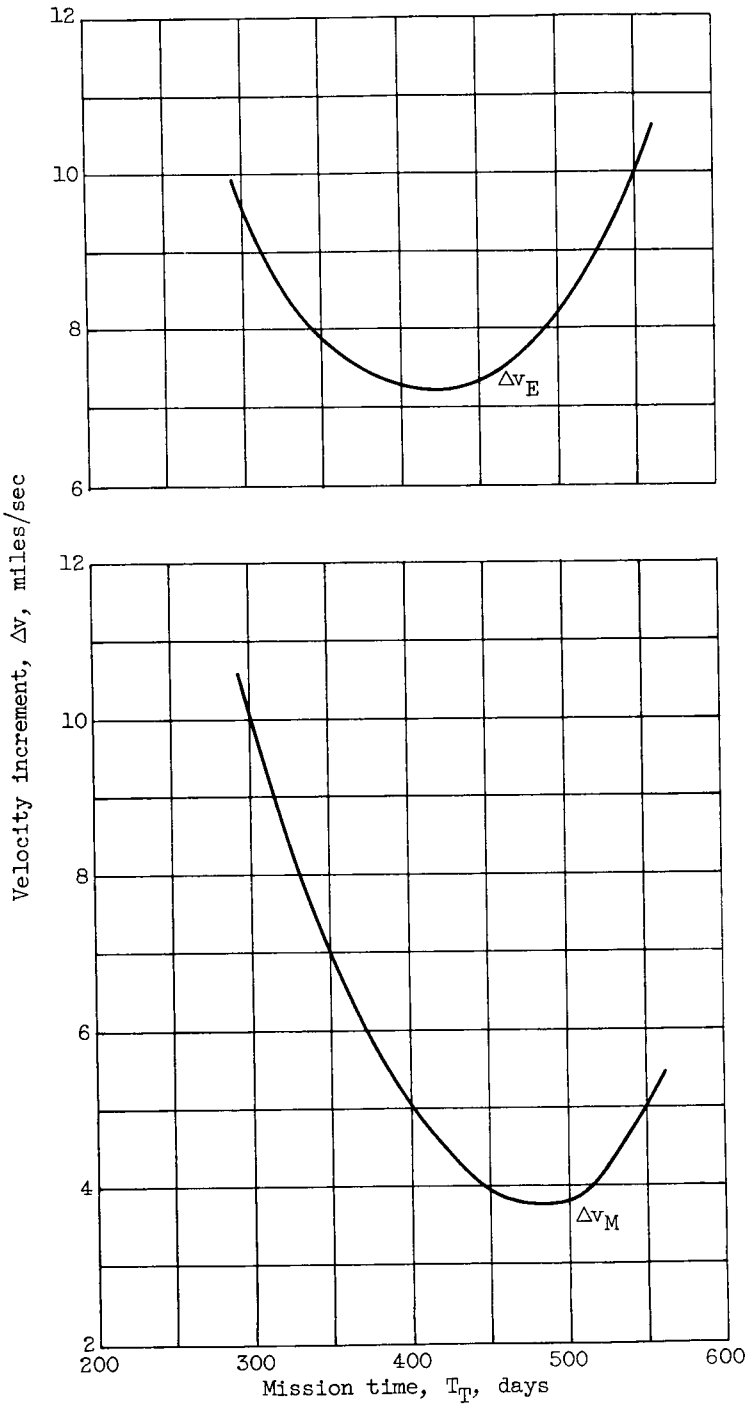


(c) Velocity increments at Earth and Mars for perihelion route.

Figure 19. - Continued. Path parameters for direct-perihelion round trips to Mars starting, waiting, and ending in circular orbits at 1.1 planet radii. Wait time in parking orbit at Mars, 100 days.

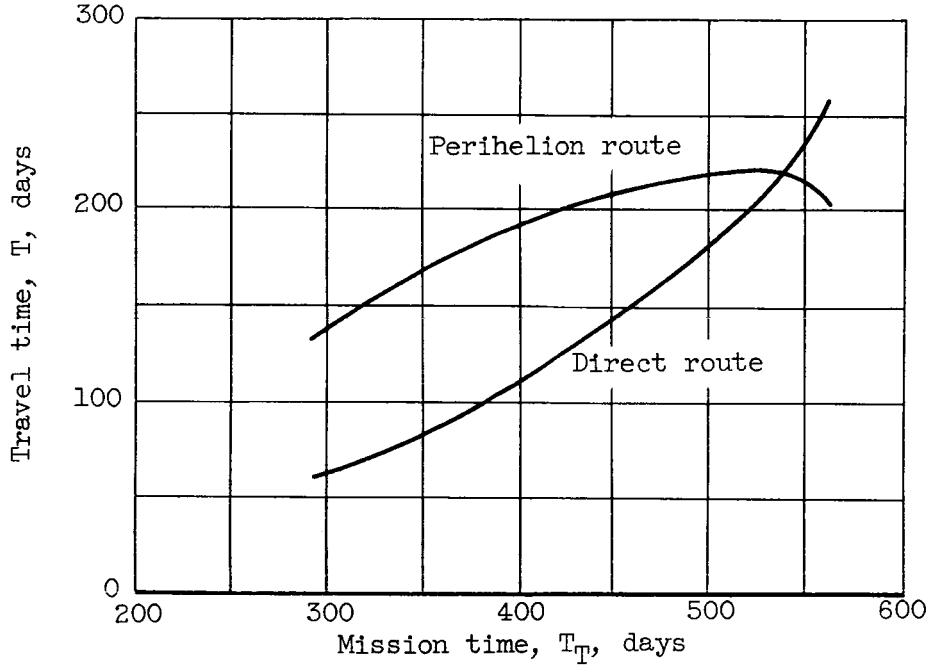


(d) Travel time.

Figure 19. - Concluded. Path parameters for direct-perihelion round trips to Mars starting, waiting, and ending in circular orbits at 1.1 planet radii. Wait time in parking orbit at Mars, 100 days.

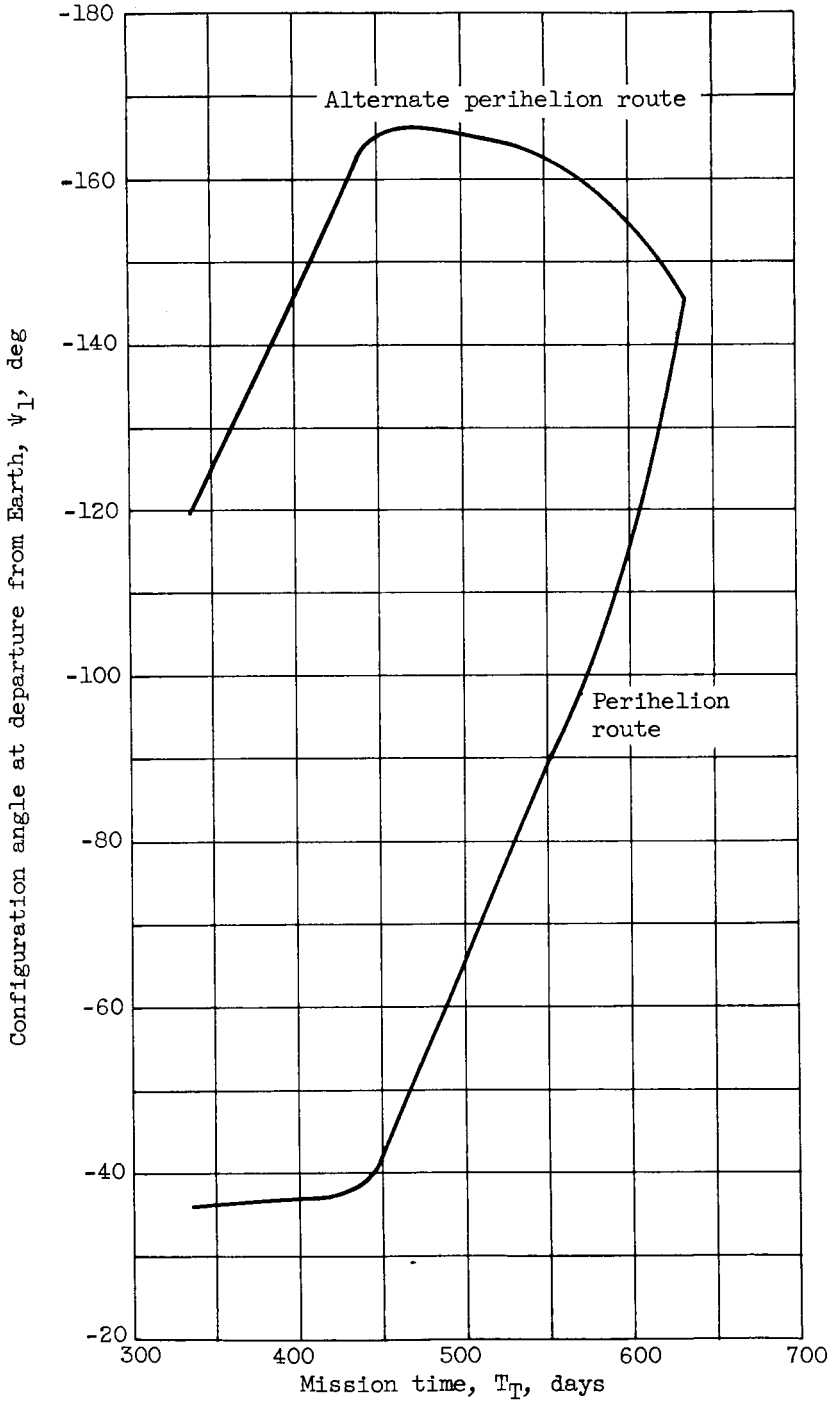


(a) Configuration angle at departure from Earth.

Figure 20. - Path parameters for perihelion-perihelion round trips to Mars starting, waiting, and ending in circular orbits at 1.1 planet radii. Wait time in parking orbit at Mars, 100 days.

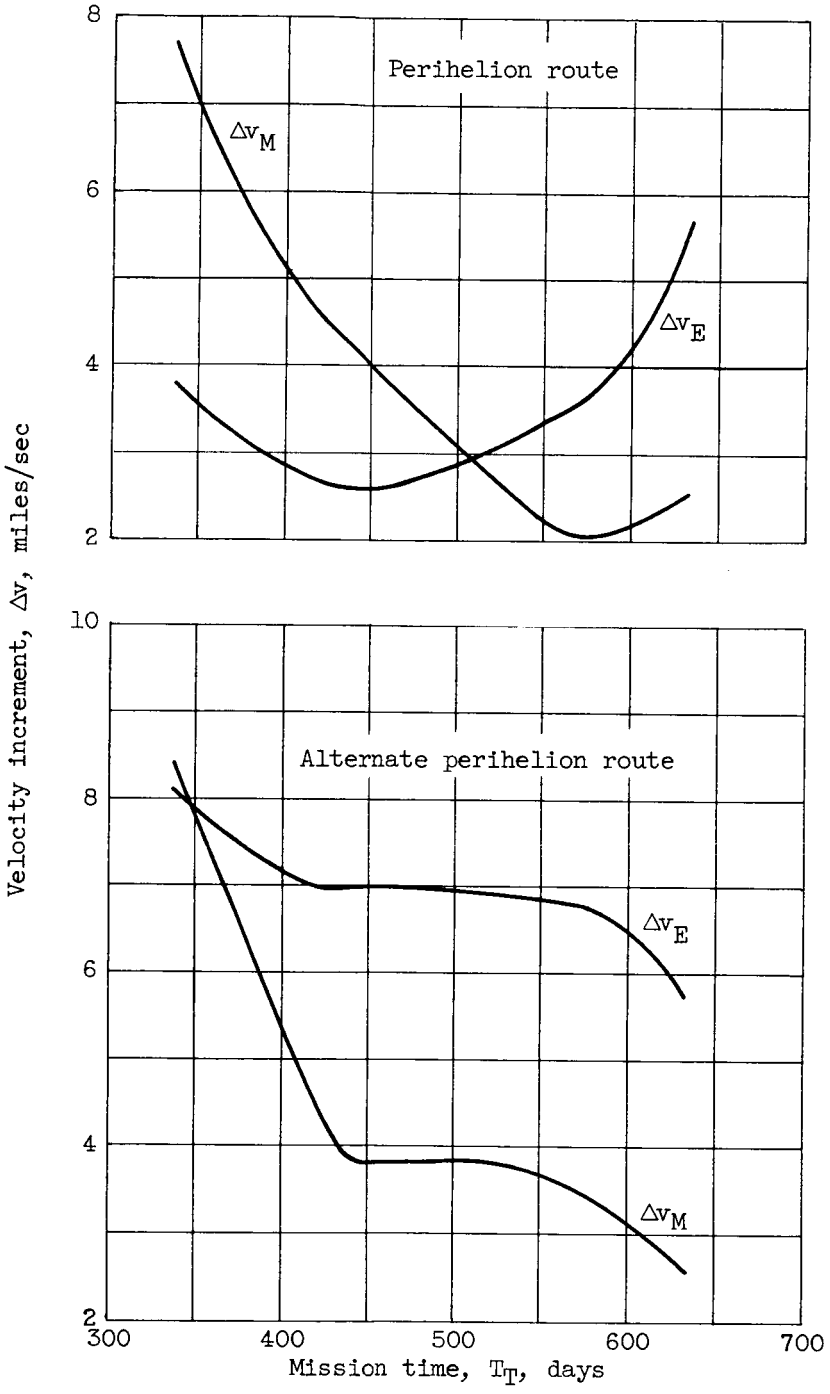


(b) Velocity increments at Earth and Mars.

Figure 20. - Continued. Path parameters for perihelion-perihelion round trips to Mars starting, waiting, and ending in circular orbits at 1.1 planet radii. Wait time in parking orbit at Mars, 100 days.

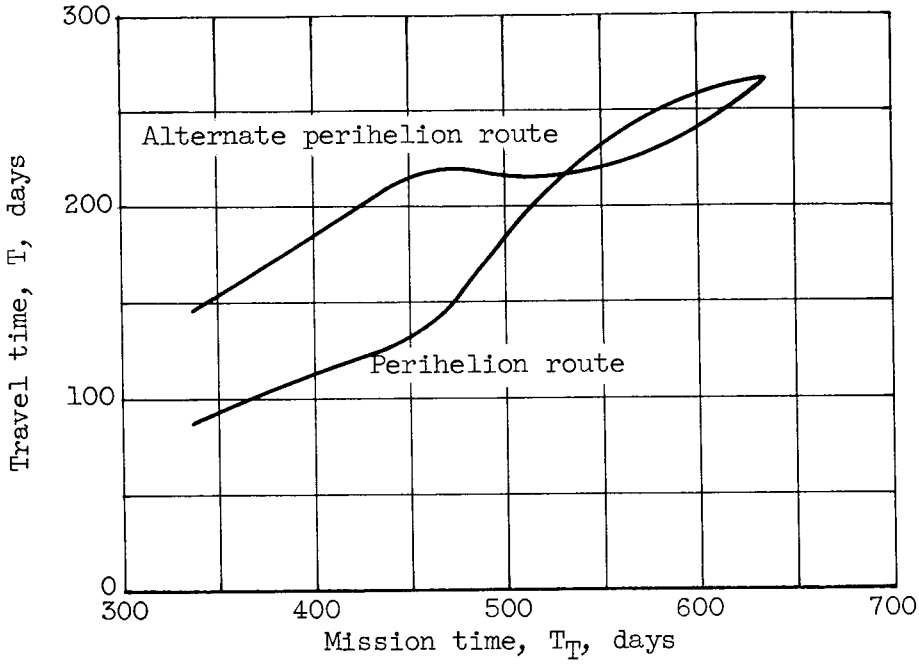


(c) Travel time.

Figure 20. - Concluded. Path parameters for perihelion-perihelion round trips to Mars starting, waiting, and ending in circular orbits at 1.1 planet radii. Wait time in parking orbit at Mars, 100 days.